Improving bio aviation fuel yield from biogenic carbon sources through electrolysis assisted chemical looping gasification

Downloaded from: https://research.chalmers.se, 2026-10-07 07:28 UTC

Citation for the original published paper (version of record):
Shahrivar, M., Saeed, M., Surywanshi, G. et al (2023). Improving bio aviation fuel yield from biogenic carbon sources through electrolysis assisted
chemical looping gasification. Fuel, 348. http://dx.doi.org/10.1016/j.fuel.2023.128525

N.B. When citing this work, cite the original published paper.

research.chalmers.se offers the possibility of retrieving research publications produced at Chalmers University of Technology. It covers all kind of research output: articles, dissertations, conference papers, reports etc. since 2004. research.chalmers.se is administrated and maintained by Chalmers Library

(article starts on next page)

Fuel 348 (2023) 128525

Contents lists available at ScienceDirect

Fuel

journal homepage: www.elsevier.com/locate/fuel

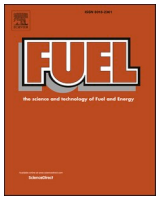

Full Length Article

Improving bio aviation fuel yield from biogenic carbon sources through electrolysis assisted chemical looping gasification

Mohammad Shahrivar [a], Muhammad Nauman Saeed [a,*], Gajanan Dattarao Surywanshi [b], Tobias Mattisson [a], Amir H. Soleimanisalim [c]

[a] Department of Space, Earth and Environment, Chalmers University of Technology, Sweden
[b] Department of Chemistry and Chemical Engineering, Chalmers University of Technology, Sweden
[c] Biorefinery and Energy Department, RISE Research Institutes of Sweden, Sweden

ARTICLE INFO

Keywords:
Chemical looping gasification
Techno-economic analysis
Aspen Plus modelling
Electro-fuel
Electrolyzers

ABSTRACT

The second-generation bio aviation fuel production via Chemical Looping Gasification (CLG) of biomass combined with downstream Fischer-Tropsch synthesis is a possible way to decarbonize the aviation sector. Although CLG has a higher syngas yield and conversion efficiency compared to the conventional gasification processes, the fraction of biogenic carbon which is converted to biofuel is still low (around 28%). To increase carbon utilization and biofuel yield, incorporation of two types of electrolyzers, Polymer Electrolyte Membrane (PEM) and Molten Carbonate Electrolysis Cell (MCEC), for syngas conditioning has been investigated. Full chain process models have been developed using an experimentally validated CLG model in Aspen Plus for Iron sand as an oxygen carrier. Techno-economic parameters were calculated and compared for different cases. The results show that syngas conditioning with sustainable hydrogen from PEM and MCEC electrolyzers results in up to 11.5% higher conversion efficiency and up to 8.1 % higher biogenic carbon efficiencies in comparison to the syngas conditioning with water gas shift reactor. The study shows that the lowest carbon capture rates are found in the configurations with the highest biogenic carbon efficiency which means up to 14% more carbon ends up in FT crude compared to the case with conventional WGS conditioning. Techno-economic analysis indicates that syngas conditioning using PEM and MCEC electrolyzers would result in an increase of the annual profit by a factor of 1.4 and 1.7, respectively, when compared to using only WGS reactors.

1. Introduction

Climate change has made it harder for both humans and wild animals to survive as global warming directly injures animals, ruins the habitats they rely on for survival, and has a disastrous impact on people's way of life and communities [1]. Since the beginning of the industrial revolution, carbon dioxide emissions, which are mostly caused by the burning of fossil fuels have increased tremendously [2]. The carbon budgets for the 1.5 °C and 2 °C global warming limitations would run out soon if current emissions of roughly 40 $GtCO_2$/year remain unaltered. Therefore, there is a need to cut CO_2 emissions swiftly and dramatically [2]. Most Intergovernmental Panel on Climate Change (IPCC) emission scenarios that adhere to the global two-degree limit call for the deployment of carbon capture and storage (CCS) for key industrial sectors because over 80% of present primary energy usage is still dependent on fossil fuels [3].

The EU transportation sector's greenhouse gas emissions increased steadily between 2013 and 2019, which is a pattern that stands out clearly from those of other sectors. Due to decreased activity during the Covid-19 pandemic, the statistics for 2020 showed a significant fall in transport emissions. After 2020, it is predicted that the domestic and international transportation emissions would rebound and increase again; however, with additional measures adopted by the EEA member states recently, the domestic emissions are anticipated to drop to the 1990 level in 2029. However, emissions from aviation and maritime transport are expected to rise continuously in the future [4]. In 2021, aircraft transport contributed more than 2% of the world's energy-related CO_2 emissions, growing more quickly recently than cargo, rail, or road [5]. Unlike road or rail sector which has the option to be electrified, finding alternative fuel for the aviation industry to reduce the CO_2 emissions from this sector is not feasible at the current development stage of the technologies [6]. Therefore, green fuels are needed for the

* Corresponding author.
E-mail address: mnauman@chalmers.se (M.N. Saeed).

https://doi.org/10.1016/j.fuel.2023.128525
Received 23 January 2023; Received in revised form 11 April 2023; Accepted 23 April 2023
Available online 5 May 2023
0016-2361/© 2023 The Author(s). Published by Elsevier Ltd. This is an open access article under the CC BY license (http://creativecommons.org/licenses/by/4.0/).

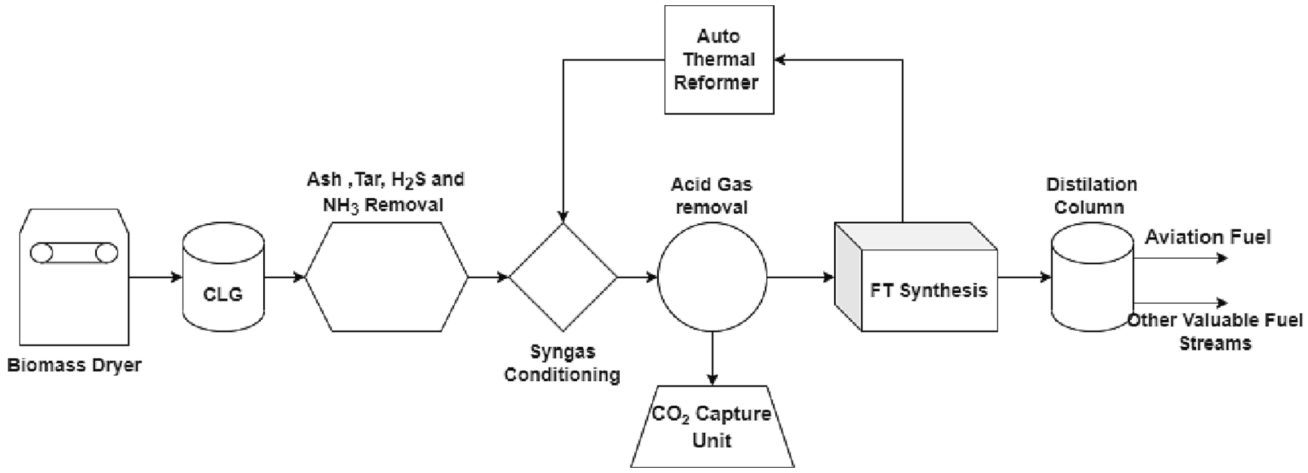

Fig. 1. Full chain process concept for biomass fuel production using CLG.

aviation sector to reduce its carbon emissions. In contrast to other renewable energy sources, biomass may be converted directly into liquid fuels, or "biofuels," to help supply the need for transportation fuel. Since the same amount of CO_2 will be consumed during the production of biomass, the GHG emissions from the burning of biofuels will not increase the quantity of CO_2 in the atmosphere [7].

To limit global warming to 2 °C before the end of this century, negative emission technologies need to be deployed to capture CO_2 from the atmosphere [3]. Negative CO_2 emissions may be accomplished by combining the use of biomass with carbon capture, or BECCS to produce bio-aviation fuel. A potential strategy for decarbonizing industries like aviation involves chemical looping gasification (CLG) of biomass in conjunction with downstream Fischer-Tropsch (FT) synthesis, as explained in Saeed et al. [8]. The CLG of biomass is a novel indirect gasification-based alternative that improves energy efficiency and simplifies the process of producing renewable hydrogen, synthetic fuels, or chemicals while confining CO_2 emissions and reducing the work needed to capture CO_2 [9]. In order to create hydrocarbon products, synthesis gas comprising hydrogen and carbon monoxide must first undergo a process known as Fisher-Tropsch synthesis [10]. Syngas conditioning before the FT reactor is essential since the process calls for a certain condition of syngas. This condition is defined by the H_2/CO molar flow rate ratio which needs to be around 2.1 [10]. Water Gas Shift (WGS) reactor is one way to condition this ratio in the syngas before the FT synthesis process. By using catalysts made of iron or cobalt, the syngas is transformed into hydrocarbons in the highly exothermic FT synthesis process [10]. The process configuration for bio-aviation fuel production can be seen in Fig. 1.

For the purpose of producing syngas, the biomass is first dried in a biomass drying unit before going through a CLG plant. The syngas passes through a number of cleaning devices where solid particles, tars, hydrogen sulfide, carbon dioxide, ammonia, and nitrogen get captured. The syngas conditioning unit is required to adjust the H_2/CO ratio. The CO_2 in the flue gas is captured before FT synthesis and send to CO_2 capturing unit. By using the "Anderson Schultz Flory" distribution in the FT reactor, the syngas is transformed into hydrocarbons. The FT crude produced by the FT reactor is made up of hydrocarbons with various carbon numbers and chain lengths. While the heavier hydrocarbons are sent to an atmospheric distillation column, the lighter hydrocarbons in the gaseous phase are sent to an auto thermal reformer to be converted back to syngas before mixing with the clean syngas from the syngas cleaning unit to improve the yield of heavier hydrocarbons in the FT crude.

Although the technologies for bio-aviation fuel production are available, providing sustainable biomass for biofuels is not a promising task as biomass supply for future usage is limited. According to Panoutsou [11], the supply of biomass for bioenergy will be constant between the years 2030 and 2050, despite estimates for the total quantity of biomass that will increase for all markets from 0.98 to 1.3 Mtoe dry tons of biomass. It means that there will not be as much biomass available for making biofuel if the demand for biofuels rises. The potential for biomass supply will stay similar and constant for the energy sector during this period due to [11]:

1- Rules and regulations for the sustainable use of land and water resources proposed a 30% decrease in the agricultural area by 2050 in the EU.
2- Improvements in forest management are gradual due to the long growing cycles of forests, which prevent quick changes in potential growth.
3- Awareness of the need to reduce waste and more stringent rules and standards for recycling.

These logistic and political barriers for providing biomass for bio-aviation fuel production suggest that the biogenic carbon from the biomass should be conserved in the process to maximize the yield of biofuel production. In other words, the carbon conversion from biomass to biofuel should increase to save biogenic carbon.

One possible way to decrease the carbon losses is limiting the syngas conditioning activity in the BtL process by using power to gas technologies. In order to store intermittent renewable energy in the form of chemical fuels such as hydrogen, methanol and methane, technologies like power-to-gas and power-to-liquid systems based on electrolysis are being evaluated [12–14]. Power to gas methods enable the production of gas, which can be easily stored, transported, and transformed into other useful chemicals [15].

This study investigates improving the biogenic carbon efficiency for the bio-aviation fuel production by conditioning the syngas with hydrogen produced from electrolysis rather than using WGS reactors where some CO gets converted to CO_2. The study was conducted using a validated CLG model in Aspen Plus process simulation software [8], where the complete chain process models of biomass to liquid fuel (BtL) using iron-sand as the oxygen carrier (OC) and two types of electrolyzers (both mature and lab scale electrolyzer technologies) for syngas conditioning were created. In this way, the ultimate utilization of carbon could be increased, increasing production of condensable fuel.

In addition to the novelty in the integration of electrolyzer technology in BTL through use of CLG, this study is also novel as it investigates using iron sand as an oxygen carrier (OC) in CLG for biofuel production. Iron sand is a slag from copper smelters and is produced in enormous amounts in Sweden [16]. The study aimed to evaluate the feasibility of valorizing this waste material in BtL which brings environmental and

Table 1
List of CLG pilot plants.

Pilot plant	Capacity	Oxygen carrier	Reference
Instituto de Carboquímica (ICB-CSIC), Zaragoza, Spain	50 kW_{th}	Ilmenite	[24]
Southeast University, Nanjing, China	25 kW_{th}	Natural Hematite	[25]
Chalmers University of Technology, Gothenburg, Sweden	10 kW_{th}	LD slag[1] and Ilmenite	[26,27]
Instituto de Carboquímica (ICB-CSIC), Zaragoza, Spain	1.5 kW_{th}	Fe_2OAl, Ilmenite, LD slag	[17,28]

[1] LD slag is one of the recyclable wastes produced by basic oxygen furnaces (BOF) or Linz-Donawitz (LD) converters in integrated steel plants.

Table 2
Syngas purity needed for FT synthesis [31].

Component	Needed Purity
H_2S COS	$H_2S + COS + CS_2 < 1$ ppm
HCN NH_3	$HCN + NH3 < 1$ ppm
Alkalis	$HF + HCl + HBr < 0.01$ ppm
Halides	< 0.01 ppm

economic benefits and promote circular economy.

For the gasification of solid fuels, like biomass, chemical looping gasification (CLG) is a cutting-edge method. Two connected fluidized bed reactors make up the conventional reactor system, in which solid metal oxide particles, or oxygen carriers, are circulated between the two fluidized bed reactors. These materials transport the oxygen needed for the endothermic gasification reaction in addition to sensible heat needed for sustained autothermal operation. The reactors are called Fuel reactor (FR) and Air reactor (AR). The biomass is initially devolatilized in the fuel reactor (fluidized with steam and/or carbon dioxide), resulting in char (C), ash, and volatiles, primarily CH_4, CO, H_2, CO_2, H_2O, H_2S, NH_3, and higher hydrocarbons (tars) [17].

$$Biomass \rightarrow Char + Volatile\ gases\ (H_2 + CO + CO_2 + H_2O + CH_4) + Tar \quad (1)$$

The gasification agent converts the char into CO and H_2 through the reactions below:

$$C + H_2O \rightarrow CO + H_2 \quad (2)$$

$$C + CO_2 \rightarrow 2\,CO \quad (3)$$

The conversion of H_2O via the water–gas shift reaction results in the formation of H_2:

$$CO + H_2O \leftrightarrow CO_2 + H_2 \quad (4)$$

By reducing the oxygen carrier, the gaseous byproducts of devolatilization and gasification, primarily CO, CH_4, and H_2, are partially oxidized producing heat for autothermal operation of the FR:

$$Me_xO_y + CO \rightarrow Me_xO_{y-1} + CO_2 \quad (5)$$

$$4\,Me_xO_y + CH_4 \rightarrow 4\,Me_xO_{y-1} + CO_2 + 2\,H_2O \quad (6)$$

$$Me_xO_y + H2 \rightarrow Me_xO_{y-1} + H_2O \quad (7)$$

The oxygen carrier particles are separated from the syngas leaving the fuel reactor (using a cyclone separator) and delivered to the air reactor (fluidized with air), where the oxygen in the air re-oxidizes the reduced form of the oxygen carrier Me_xO_{y-1} to Me_xO_y:

$$Me_xO_{y-1} + 0.5\,O_2 \rightarrow Me_xO_y \quad (8)$$

While the total reaction in the FR is endothermic, the reaction in the AR is substantially exothermic. Heat is transferred from the solids flowing from the AR, which is operated at a higher temperature (900–1050 °C), to the FR, in order to maintain a temperature of around 850–950 °C [18]. A fraction of the syngas should also be combusted in the fuel reactor to achieve autothermal operation [19].

Although there are similarities between the Indirect gasification (IG) and CLG process, there are some clear differences. IG normally utilizes sand as bed material where the main aim is bio-methane production. On the other hand, CLG uses oxygen carriers as bed material, and the aim is syngas production. The use of oxygen carriers changes the fuel conversion process substantially, and thus the heat balance and process streams are totally different. In CLG, the majority of CO_2 is ideally limited to the Fuel Reactor (FR), where it is available for carbon capture, in contrast to the IG process, which utilizes fuel in the "air" reactor in order to supply heat to the particles. Hence, CO_2 is released in the air reactor in IG where it is highly diluted with nitrogen. In CLG, the air reactor is ideally clean, and any CO_2 is found together with the syngas in the FR. As a result, CLG would enable lower costs for gas purification and carbon sequestration. Compared to the conventional indirect gasification, CLG has various benefits [20–22]:

- A greater partial pressure of CO_2 and H_2O in the fuel reactor than in the conventional indirect gasification and oxygen transfer by OC, which results in a more oxidizing environment.
- The oxygen carrier's catalytic properties lead to a greater syngas yield and a lower tar concentration in the syngas.
- Less alkali emissions from the air reactor compared to fuel reactor which makes the gas cleaning steps less extensive
- No need for an expensive, energy-intensive air separation unit (ASU).

The continuous CLG operation has been successfully demonstrated in a number of pilot-units with capacities ranging from 1.5 kW_{th} to 50 kW_{th}, where different Fe- and Mn- based oxygen carriers have been used. It is clear that the process can work well with high yield of syngas from the fuel reactor [22,23]. Table 1 summarize the pilot plant CLG tests at different institutes. It is clear that the process can work well with high yield of syngas from the fuel reactor.

There are many downstream processes that use catalysts to operate which are sensitive to poisonous materials in the syngas. Gas cleanup procedures are therefore necessary but have a big impact on plant economics because they can account for a lot of the capital and operational costs [29]. The syngas cleaning unit contains several stages such as fly ash removal unit, tar removal unit and acid gas removal units which are explained by Arvidsson et al. [30] in detail. The syngas cleaning requirements for FT synthesis can be seen in Table 2.

The syngas composition before the FT reactor should match specific requirements, such as the H_2/CO ratio (~2.1) and the syngas cleaning conditions stated in the previous section, for the optimum conversion of syngas to produce biofuel [10]. This paper studies two method for conditioning syngas to reach the desired target:

1- Water Gas shift reactor (WGS)
2- Electrolysis

WGS is a traditional method of adjusting the H_2/CO molar ratio. H_2/CO ratio can be adjusted by the conditioning unit before the FT reactor. The specific ratio, which depends on product type and catalyst, can be controlled by the water–gas shift reactor. Water-gas shift reaction is an exothermic reaction that forms as below:

$$CO + H_2O \rightarrow CO_2 + H_2 \quad (9)$$

The temperature is governing which direction the reactions happen, generally low temperatures promote CO conversion thermodynamically, while pressure has little influence because the process is exothermic and has no mole number variation [32]. The H_2O/CO feed

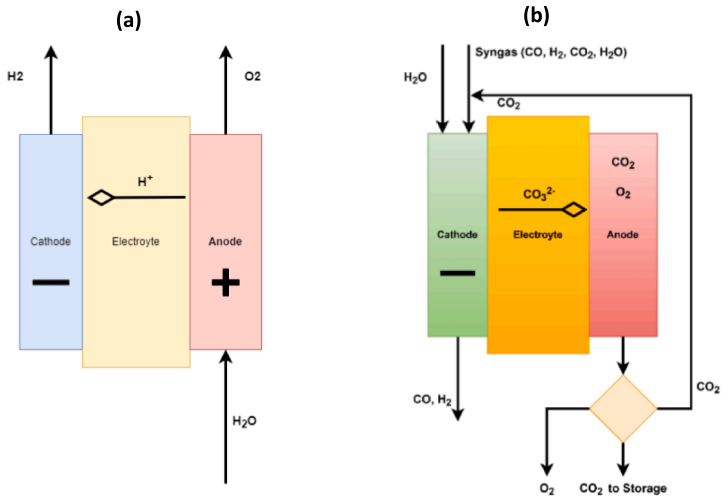

Fig. 2. Working principle of (a) PEM electrolyzers (b) MCEC electrolyzers.

molar ratio typically ranges from 2 to 5 to change the thermodynamic equilibrium conversion and control the reaction rate in the water gas shift reactor [32].

The share of energy production from renewable sources (especially wind power and hydropower) rose by 3% in 2020 compared to 2019 [33]. This rise in renewable sources indicates more curtailment of electricity production in the future to ensure the stability of the grid and system as a whole (frequency and voltage control). This curtailment of electricity in wind farms especially can be reduced by consuming electricity for the production of hydrogen in electrolyzers during hours of high net electricity production [34]. It is proposed to produce hydrogen from green electricity and introduce it for conditioning the syngas to the optimum H_2/CO molar ratio and producing bio-aviation fuel, consequently transferring more carbon from biomass to the condensable fuel [35].

This study explores feasibility of polymer electrolyte membrane (PEM) electrolysis and molten carbonate electrolysis cell (MCEC) electrolysis usage to enhance the biofuel production in the biofuel production process. Fig. 2 shows the working principles of PEM and MCEC electrolyzers.

PEM water electrolysis is one of the most promising methods, which is at Technology Readiness level (TRL) 6–8 [36], for producing high-purity, cost-effective hydrogen from renewable energy sources because it produces oxygen as the only byproduct and emits no carbon. Additionally, the hydrogen (H_2) and oxygen (O_2) produced are directly employed in the process and other industrial uses [37].

At the relevant electrodes, such as the cathode for hydrogen and the anode for oxygen, hydrogen and oxygen are electrochemically separated from water in PEM water electrolysis. PEM water electrolysis is started by pumping water to the anode, where it separates into oxygen (O_2), protons (H^+), and electrons (e^-). The proton conducting membrane transports these protons to the cathode side. The external power circuit, which supplies the reaction's driving force (cell voltage), allows the electrons to leave the anode. The hydrogen is created at the cathode side by the recombination of protons and electrons [37].

$$Anode: H_2O \rightarrow 2H^+ + \frac{1}{2}O_2 + 2e^- \quad (10)$$

$$Cathode: 2H^+ + 2e^- \rightarrow H_2 \quad (11)$$

$$Overall\ reaction: H_2O \rightarrow H_2 + \frac{1}{2}O_2 \quad (12)$$

PEM water electrolysis has many benefits, including its compact design, high current density (above 2 A/cm^2), high efficiency, quick response, small footprint, ability to operate at lower temperatures (20–80 °C), ability to produce ultrapure hydrogen as well as oxygen as a byproduct, and ease of balancing. These factors make PEM electrolysis plants more appealing for use in industrial applications [38].

MCEC which is at TRL level 3, makes it possible to produce fuel gases, such as hydrogen or syngas, by removing CO_2 from the syngas stream and increasing the viability of CO_2 capture [14]. Most of the commercially available electrolysis technology is designed to operate at low temperatures, such as in alkaline water electrolysis and proton exchange membrane water electrolysis. However, experimental studies have demonstrated that the thermodynamic and kinetic characteristics of the electrochemical process are advantageous in the high-temperature electrolysis of MCEC [39].

The reactions happening in MCEC are expressed below:

$$Cathode: H_2O + CO_2 + 2e^- \rightarrow H_2 + CO_3^{2-} \quad (13)$$

$$H_2O + CO \rightarrow H_2 + CO_2 \quad (14)$$

$$Anode: 2CO_3^{2-} \rightarrow O_2 + 2CO_2 + 4e^- \quad (15)$$

As an electrolyte, molten alkali metal carbonate salts are frequently used in MCEC, which requires operating temperatures between 600 and 800 °C [39]. Due to the higher solubility of CO_2 in the molten carbonate electrolytes, this technology is more preferred in CO_2 utilization concepts compared to other high temperature electrolysis technologies like solid oxide electrolysis cell (SOEC). Separating of the CO_2 and O_2 allows for their utilization. The generation of H_2 increases by recycling the CO_2 back into the cathode, while the O_2 can be used in the gasification or auto thermal reformer processes. Furthermore, through the water gas shift (WGS) reaction, the CO content in the cathode's output stream can be adjusted, making it possible to regulate the H_2/CO ratio [14].

The technique of converting biomass into liquid fuel, or BtL, has been around since the 20th century, when Germany invented it to make liquid fuel from its coal reserves [40]. Spyridon Achinas looked into the technological and economic viability of producing sustainable aviation fuel, and the results showed that as of today, no industrial technique could economically compete with the costs of traditional jet fuel. On the other hand, policymaking could benefit the bio-jet fuel industry by funding more into the research to lower the production costs [41]. For a comprehensive assessment of the current status of thermochemical conversion techniques used to produce biofuels from lignocellulosic biomass, reader can refer to study that has been investigated by Paola Ibarra-Gonzalez et al. [42].

One popular technique for transforming syngas into liquid fuel is the

Table 3
Base case model conditions.

Parameters	Assumptions
Biomass Fuel	Forest Residue (Finland)
Raw Biomass Moisture Content	50 %
Biomass Moisture Content After Drying	15 %
Gasification Steam Temperature	500 °C
Oxygen carrier	LD slag
Fuel Reactor Temperature	935 °C
WGS Reactor Temperature	350 °C
Optimum H_2/CO Ratio for FT Synthesis [10]	2.1
Fischer Tropsch Synthesis Temperature	220 °C
Auto-thermal Reformer Temperature	1000 °C
Auto-thermal Reformer Steam Temperature	250 °C

Table 4
Selected biomass composition.

Forest residue in Finland	
HHV (MJ/kg d.b*)	20.67
Proximate analysis (wt. % d.b*)	
Volatile Matter	79.3
Fixed Carbon	19.37
Ash	1.33
Ultimate analysis (wt. % d.b*)	
C	51.3
H	6.1
O	0.4
N	40.85
S	0.02
Ash	1.33

* d.b. stands for dry basis.

Fischer-Tropsch Synthesis (FTS) process. The catalytic FT synthesis creates a variety of hydrocarbons from syngas, which is mostly composed of hydrogen (H_2) and carbon monoxide (CO). In the FTS sections, it is crucial to consider the operating mode, the kind of catalyst used, and the reactor design. These process factors control the syngas conversion efficiency as well as the product distribution of the inputs for the product upgrading section. High-Temperature Fischer-Tropsch (HTFT) or Low-Temperature Fischer-Tropsch are the two possible operational modes (LTFT). The Anderson-Schulz-Flory (ASF) definition can be used to describe the distribution among these several carbon ranges. The output of the ASF model is an ideal distribution that forecasts the FT process's end products. The molar fraction (Mn) of the hydrocarbon product with carbon number (n) is simply reliant on the chain growth probability (α), which is a function of the rates of chain growth and chain termination [43,44].

$$M_n = \alpha^{n-1}(1-\alpha) \tag{16}$$

The chain growth probability (α) is based on the experimental investigation and reported by Song as below [45]:

$$\alpha = \left(A * \frac{\gamma_{CO}}{(\gamma_{CO}+\gamma_{H2})} + B\right) * [1 - 0.0039(T-533)] \tag{17}$$

where the T is the operating temperature in Kelvin and A and B are constants reported by [45] to be 0.2332 ± 0.0740 and 0.6330 ± 0.0420, respectively. The FTS is an exothermic process in which the operational temperature is controlled with a continuous supply of cooling water. The operational pressure is normally between 20 and 30 bar.

2. Methodology

This section covers the methodology to construct BtL process models in Aspen Plus with and without hydrogen conditioning from electrolysis. The procedure for techno-economic analyses as well as the required assumptions have also been explained.

2.1. Methods of modelling and techno-economic analysis

The set of conditions and assumptions for modelling the BtL plant with syngas conditioning using WGS reactor (base case) are shown in Table 3.

Condori et al. [17] found a char conversion of 98.7% in FR at 930 °C and a steam-to-biomass ratio of 0.62. Therefore, considering the experimental data in the literature for the high temperatures and steam-to-biomass ratios, which are the case in this work, the char conversion in the FR is assumed to be 99%. For purposes of simplification, the system has also been modelled with no pressure losses; nevertheless, the capital costs of the compressors required to compensate for the pressure loss have been considered in the techno-economic analysis.

2.1.1. Biomass

In this work, forest residues are used as fuel for the process, which has an LHV between 8 and 9 MJ/kg (as received) and a moisture content of 50% [46,47]. The fuel must be processed to improve the quality of the syngas, which will affect the plant's thermal and chemical efficiency. The forest residue is dried to reduce the moisture level of the raw biomass fuel to 15%. The plant's low-temperature waste heat is used to generate drying heat. According to Hannula et al. [47], problems with energy efficiency, GHG emissions, heat integration, and dryer performance make it difficult to dry biomass to low levels of moisture. In order to produce synthesis gas, feedstocks must be dried to a moisture content of less than 30%, ideally less than 15%, and in the case of pyrolysis, less than 10%.

The ultimate and proximate analysis of the typical forestry residue in Finland is presented in Table 4 [48] which is also the gasification fuel in this investigation.

2.1.2. Oxygen carrier

The model has been tested using iron sand, a byproduct of the copper industry, as oxygen carrier. Iron sand is a crystalline iron silicate aggregate from the copper smelter (copper smelter slag) [16]. Iron sand has been selected for this study due to its low oxygen-carrying capacity making it a suitable choice for CLG and Chemical Looping Reforming (CLR). This material is produced in enormous amounts in Sweden and Europe with very low cost and available value chains, and there has been no previous process study with this material [49]. It is expected that the oxygen carrier transformations would occur only via the Fe_2O_3-Fe_3O_4 redox transition, although in reality, lower forms of iron oxides, like FeO, could also be formed in the fuel reactor. Also, it has a size distribution of between 63 and 560 μm which is in the proper range for fluidized bed application, hence there is no need for crushing and sieving [16]. Also, utilizing a waste stream from the copper industry as an OC, lower the cost of the process and promote a circular economy. Table 5 lists the elements that make up iron sand.

2.1.3. Formation of tar and methane

The validated CLG process model developed by Saeed et al. [8] in which LD slag was used as the OC, has been modified for use with iron sand. Since there is no experimental data for CLG tests using iron sand as and OC, assumptions are needed for the methane and tar amount in the CLG process model using iron sand. Iron sand is an iron-based OC and the iron content in iron-sand is between the iron content in ilmenite and LD slag [20]. Therefore, the experimental data for methane and tar formation from CLG tests using LD slag and ilmenite could give a hint about the tar and methane amount for CLG using iron-sand. It is generally known that the presence of calcium and magnesium inhibits tar production in biomass gasification [17,50]. However, these components are not present in the composition of ilmenite; due to similarities between LD slag and iron sand in terms of compostion, LD slag experimental data was used in this work as opposed to ilmenite. Table 6 shows the tar and methane amount in CLG test with LD slag and ilmenite at temperature of 935 °C in a 1.5 kW_{th} pilot plant [20]. Based on the results

Table 5
Selected oxygen carrier compositions.

Composition (wt.%)	Fe_2O_3	SiO_2	CaO	MgO	Al_2O_3	Zn	Cu	Mn	Cr
Iron Sand	45	35.6	6	3	7	1.5	0.9	0.6	0.4

Table 6
Methane and tar formation in CLG test with LD slag and ilmenite at temperature of 935 °C in the 1.5 kW_{th} reactor.

Oxygen Carrier	LD slag	Ilmenite
Methane	8 vol% of dry syngas	10 vol% of dry syngas
Tar	3 g/kg of dry biomass	1.5 g/kg of dry biomass

from Condori el al. (2021), the methane amount in the fuel reactor is not very sensitive to the temperature of the fuel reactor or the steam to biomass ratio for each oxygen carrier. Also, the tar amount is in the range of 3–1.5 g/kg of dry biomass. Therefore, it has been assumed that the tar amount for CLG using the iron sand is 3 g/kg of biomass and the methane is 8 vol%. In addition, based on previous studies on tar characterization from CLG operation using LD slag and ilmenite as an OC, the main tar compounds are assumed to be Phenol, Toluene, and Naphthalene [17,26].

2.1.4. Developing process models in Aspen Plus

The Peng-Robinson equation of state with Boston-Mathias modifications (PR-BM) was chosen as the property method in the process model, and the stream class was set to MIXCINC, which has three substreams: Conventional Fluids (MIXED), Conventional Inert (CI) Solid, and Non-Conventional (NC) Solid. The sub-streams "CI Solid" and "NC Solid" consist of all solid compounds with and without defined molecular weights, respectively, whereas the sub-stream "MIXED" includes all compounds in the vapor or liquid phase. In contrast to char (graphite) and OC streams, which are modelled as CI solids, biomass and ash are

Table 7
Description of BtL process configurations employing different syngas conditioning processes to improve biogenic carbon efficiency.

Cases	Syngas Conditioning Technology	Bypass Needed	Tar Removal	Carbon Capture Technology	CO_2 Recycle Rate	Fig
A	WGS Reactor	Yes	[1]RME	Rectisol (Amine Scrubber for H_2S removal)	NA	3
B	PEM Electrolysis	No	Scrubber	Amine Scrubber		4
C				Rectisol		
D	PEM Electrolysis (hydrogen also produced for assisting in gasification in FR)			Amine Scrubber		5
E				Rectisol		
F	MCEC Electrolysis	Yes		Amine Scrubber for capturing CO_2 from syngas/Rectisol for capturing CO_2 at anode	30 % of carbon dioxide produced at anode recycled back to cathode	6
G					40 % of carbon dioxide produced at anode recycled back to cathode	
H	MCEC Electrolysis	No	Tar Reformer		30 % of carbon dioxide produced at anode recycled back to cathode	7
I					40 % of carbon dioxide produced at anode recycled back to cathode	

[1] Rapeseed Methyl Ester.

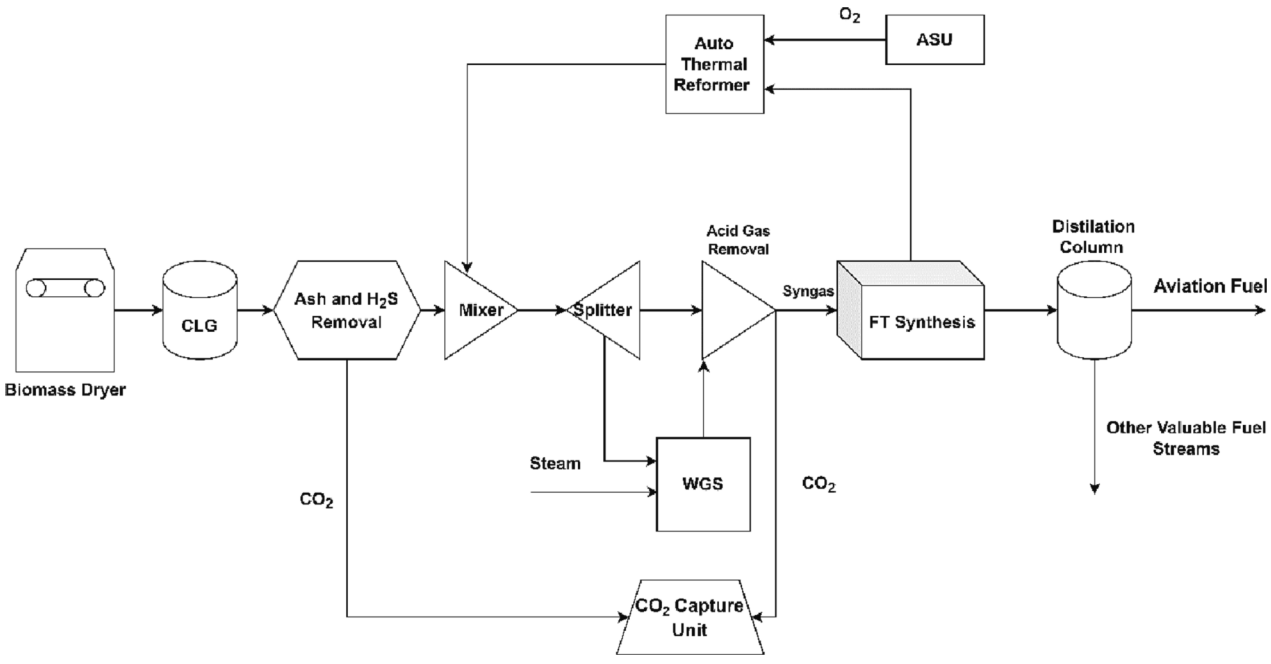

Fig. 3. Base case BtL process configuration with WGS reactor (case A) adapted from Saeed et al. [8].

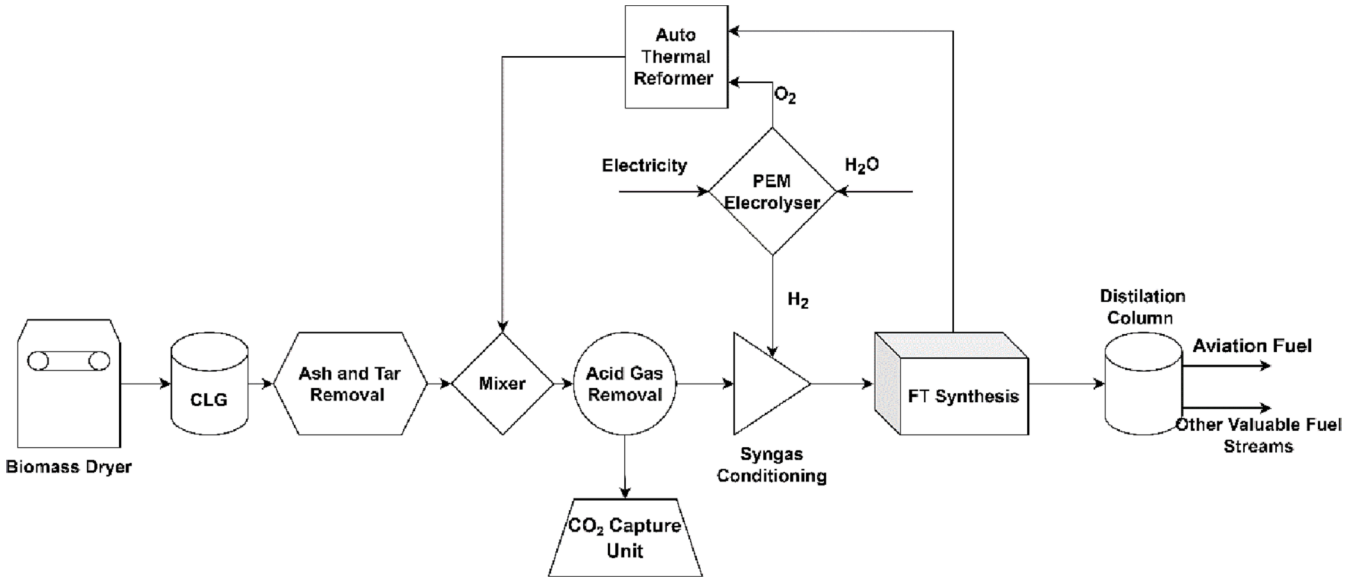

Fig. 4. BtL process with syngas conditioning using hydrogen from PEM electrolyzer (cases B and C).

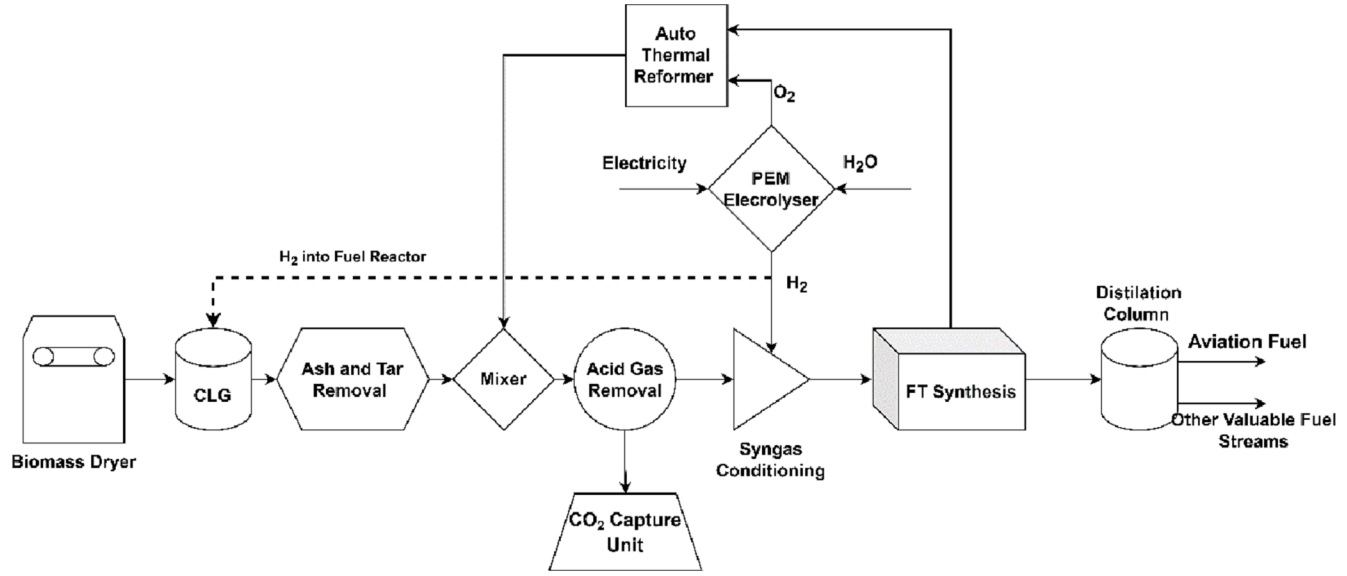

Fig. 5. BtL process with hydrogen assisted CLG and syngas conditioning using hydrogen from PEM electrolyzer (cases D and E).

specified as NC solids. The 'HCOALGEN' and DCOALIGT' property models were selected to define enthalpy and density of non-conventional solid fuel, respectively. Aspen plus software computes the enthalpy of non-conventional solid fuel using HCOALGEN property model with user-specified heat of combustion of biomass [51]. All the BtL processes, except the syngas conditioning have been modelled the same way as in Saeed et al. [8] where the model has also been validated with the experimental results using some CH_4 and tar composition inputs from experiments. Syngas conditioning unit has been modelled by modeling the PEM/MCEC electrolyzer. For simplification, PEM electrolyzer is modelled using only a stream of hydrogen, the flow of which is determined by a design specification in Aspen Plus to reach the desired H_2/CO ratio, whereas MCEC electrolyzer has been modelled using a stream of H_2O and implementing reactions (12)–(14) using design specs and calculators along with an RGibbs reactor block for simulation of WGS reaction at the cathode. A design spec block is used to achieve desired H_2/CO ratio by controlling the mass flow of steam to the electrolyzer.

2.1.5. Process configurations

Different syngas conditioning configurations of the BtL process plant for reaching the desired H_2/CO molar ratio have been studied to compare the process parameters of the models, most importantly the biogenic carbon efficiency. The base case includes WGS reactor for syngas conditioning whereas for the other cases, syngas is conditioned by mixing it with hydrogen from the electrolyzers such as PEM and MCEC. Table 7 explains the different technologies and process configurations for syngas conditioning.

Fig. 3 shows the full chain model configuration with a WGS reactor before the FT synthesis unit for syngas conditioning as explained in section 1. The syngas from cleaning unit and auto-thermal are reformer first mixed after which the stream is split to send the required fraction of syngas into the WGS reactor. Main carbon sinks are the CO_2 capture units such as Amine scrubber and Rectisol. CO_2 is mostly produced as a result of combustion and WGS reactions in the FR and later in the WGS reactor due to WGS reaction.

Syngas can also be conditioned by feeding hydrogen produced by a

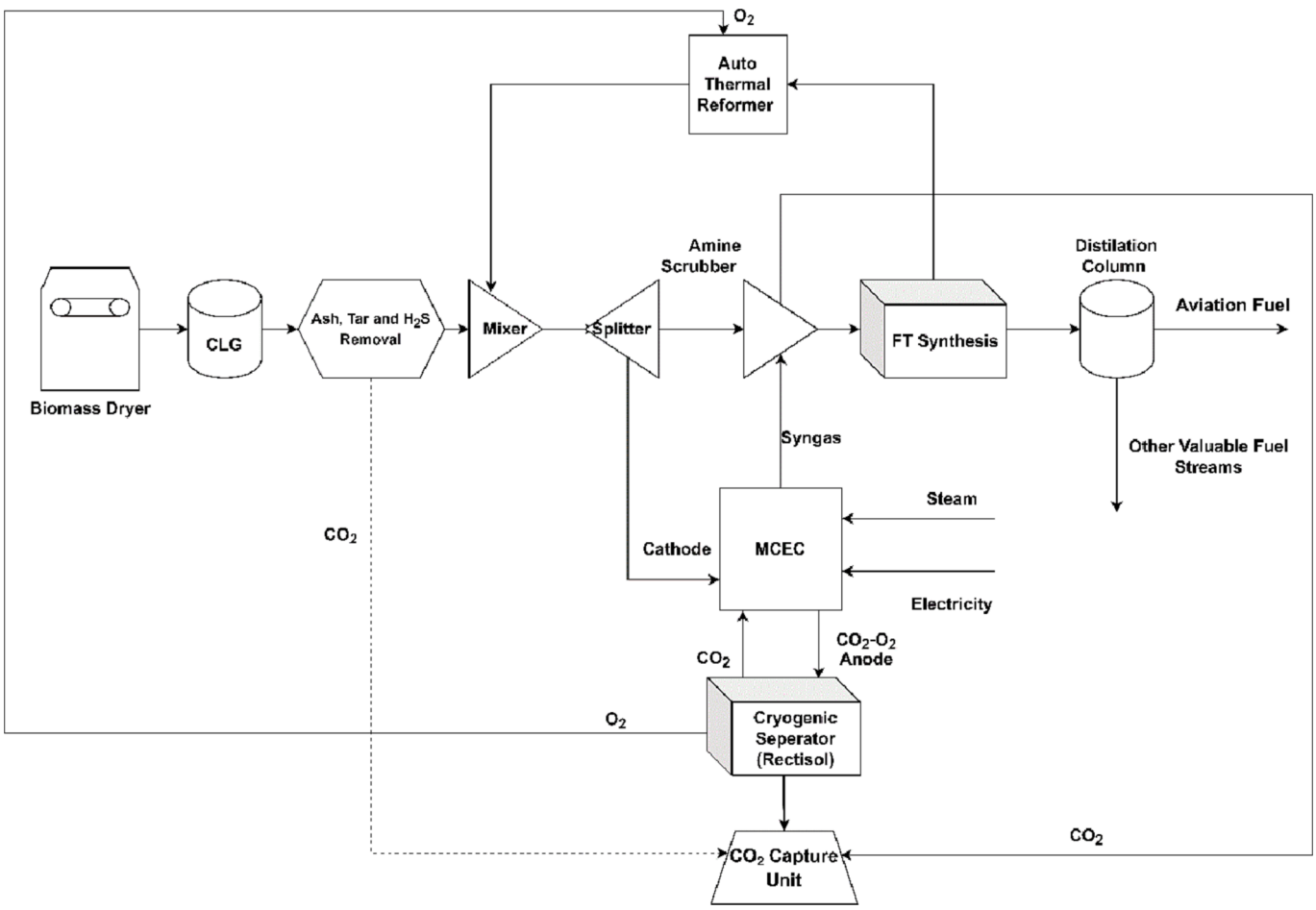

Fig. 6. BtL process with syngas conditioning using MCEC electrolyzer with bypass and internal recirculation (cases F and G).

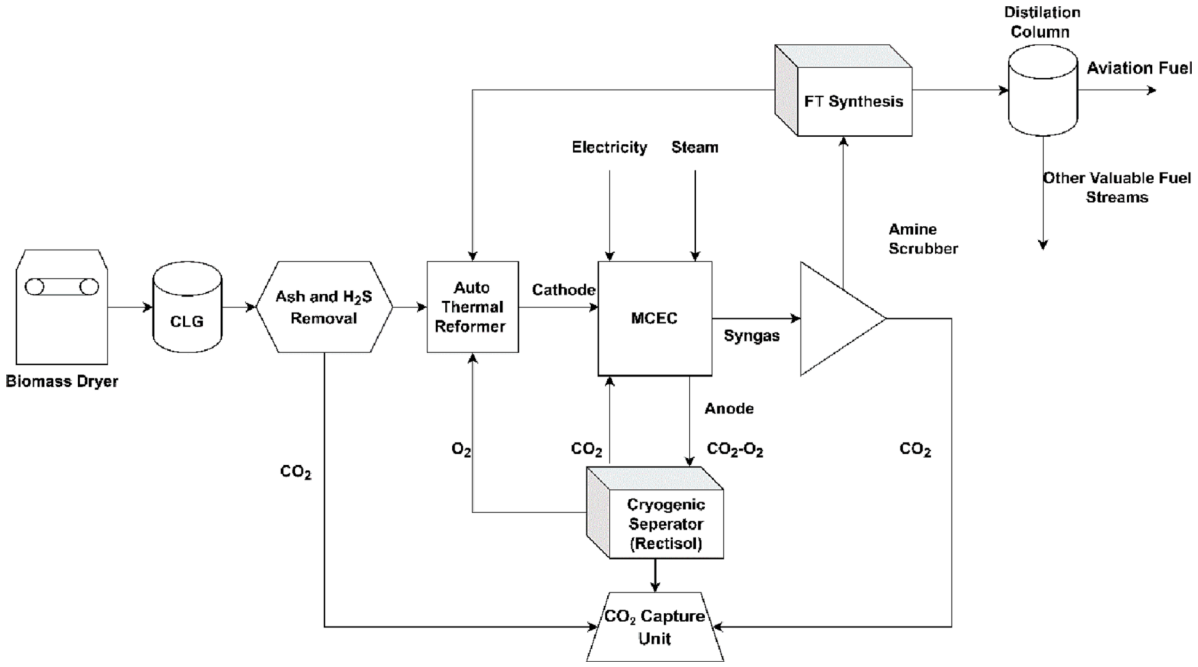

Fig. 7. BtL process with tar reformer and syngas conditioning using MCEC electrolyzer with internal recirculation (cases H and I).

Table 8
Assumptions for the techno-economic analysis of the BtL process plants.

Techno-economic Parameters	Assumptions	Reference
Economic Lifetime of Plant (yrs)	20	[8]
Discount Rate (%)	10	
Annual O&M Cost (%)	5	
Annual Operating Hours (h/yr)	8000	
Biomass Residue Chips Price (€/GJ)	5	
Electricity Price (€/GJ)	14	
District Heating Price (€/GJ)	1	
PEM Electrolyzer Efficiency (%)	58	[53]
PEM Electrolyzer CAPEX ($/kW$_e$)	1100	
MCEC Electrolyzer Efficiency (%)	77.5	
MCEC Electrolyzer CAPEX ($/kW$_e$)	2800	

Table 9
Prices of fuel assumed for the technoeconomic study.

Fuel	Price	Unit	Notes	References
Lighter Hydrocarbon Gas	5.217	$/MMBTU	Price from tradingeconomics.com for 24th March 2022	[60]
Gasoline	8.547	$/gallon	Price from GlobalPetrolPrices.com (Sweden) for 21st March 2022	[61]
Kerosene (Jet A Fuel)	144	$/bbl	Price from IATA.org (Europe and CIS) for 18th March 2022	[62]
Diesel	10.27	$/gallon	Price from GlobalPetrolPrices.com (Sweden) for 21st March 2022	[61]
Wax	1000	$/tonne	Price from paraffinwaxco.com	[63]

Table 10
Techno-economic assumptions for future scenario.

Techno-economic Parameters	Assumptions for Future Scenario
Electricity Price (€/GJ)	10
Negative Emissions Price (€/tonne CO_2)	75
PEM Electrolyzer Efficiency (%)	65.5
PEM Electrolyzer CAPEX ($/kW$_e$)	650
MCEC Electrolyzer Efficiency (%)	80.5
MCEC Electrolyzer CAPEX ($/kW$_e$)	800

PEM electrolysis cell to the syngas stream entering the FT synthesis unit as shown in Fig. 4. In this configuration the oxygen required for auto-thermal unit comes from the PEM electrolyzer; therefore, the ASU unit can be removed from the full chain process. This would mean that the conversion of CO into CO_2 in case of syngas conditioning by WGS reaction is avoided resulting in better biogenic carbon efficiency. Hydrogen from the PEM electrolyzer can also be provided to FR for better biogenic carbon efficiency since the introduction of hydrogen in FR reduces the conversion of CO into CO_2 by shifting the WGS equilibrium in FR. The configuration seen in Fig. 5 shows the implementation of hydrogen assisted gasification for a comparative analysis.

Fig. 6 shows the implementation of MCEC electrolyzer (explained in section 1) to produce hydrogen by consuming CO_2 for conditioning syngas before entering the FT synthesis unit. Rather than capturing and storing all the CO_2 produced at anode, a portion of CO_2 is recycled back to the cathode to improve the biogenic carbon efficiency and the yield of FT crude.

The split syngas stream enters the MCEC at the cathode where CO_2 in the stream reacts with steam to produce H_2 and carbonate ion. Since the temperature inside MCEC is around 800 °C, some WGS activity also happens at the cathode. The carbonate ion from cathode gets transferred to the anode where it releases four electrons and splits into CO_2 and O_2. Following the cryogenic separator where CO_2 and O_2 are separated, some CO_2 is recycled into the MCEC electrolyzer, while the rest is sent to the CO_2 capture unit. The oxygen on the other hand is also used to eliminate or reduce the oxygen demand from the ASU unit for combustion in the auto-thermal reformer.

Since tars contain long hydrocarbon chains, removing tar would result in lower biogenic carbon efficiencies. Therefore, the configuration proposed in Fig. 7 includes a tar reformer for the conversion of tar into syngas and improving the biogenic carbon efficiency compared to the base case with an RME scrubber for tar removal. In this configuration, all the syngas from cleaning section and recycled hydrocarbon from Fischer Tropsch synthesis passes through a tar reformer to produce tar free syngas. Later, all the syngas passes through the MCEC electrolyzer.

2.2. Technical parameters

The performance of all the cases given in the previous section are compared based on cold gas efficiency, conversion efficiency and biogenic carbon efficiency. These process parameters are given below:

2.2.1. Cold gas efficiency

The cold gas efficiency (CGE), which may be stated as a percentage, is defined as the efficiency of the gasification unit and is given as [52]:

$$CGE = \frac{mass\ flowrate\ of\ clean\ syngas * LHV\ of\ clean\ syngas}{mass\ flowrate\ of\ biomass\ (as\ received) * LHV\ of\ biomass\ (as\ received)} \quad (2.1)$$

2.2.2. Conversion efficiency

Conversion efficiency (CE) can be defined as the efficiency of the overall BtL process and is given:

$$CE = \frac{mass\ flowrate\ of\ FT\ crude * HHV\ of\ FT\ crude}{mass\ flowrate\ of\ biomass\ (as\ received) * HHV\ of\ biomass\ (as\ received)} \quad (2.2)$$

2.2.3. Biogenic carbon efficiency

Biogenic carbon efficiency (CCE) is defined as the ratio of the moles of carbon that end up in FT crude to the moles of carbon in the biomass. CCE is given as:

$$CCE = \frac{molar\ flowrate\ of\ \boldsymbol{C}\ in\ FT\ crude}{molar\ flowrate\ of\ \boldsymbol{C}\ in\ the\ biomass} \quad (2.3)$$

2.3. Economic analysis

This section covers common cost metrics for evaluating capital costs, operating costs, revenues, and financial measurements, as well as detail the important calculations based on the study by Hannula et al. [46] Saeed at al. [8]. Table 8 summarizes the underlying assumptions in the techno-economic study.

Smaller equipment such as compressors for pressure loss makeup, pumps, and heat exchangers are expected to cost 10% of the Total Plant Investment (TPI) [8]. The case studies' operations and maintenance (O&M) costs are taken as 5% of TPC based on Saeed et al.'s [8] study. Personnel costs (0.5%), maintenance and insurance (2.5%), oxygen carrier makeup (1%) catalysts and chemicals (1%) are all considered to be part of the operations and maintenance cost. Based on the studies available in the literature [8,14,47,54], the biomass residue and electricity cost are predicted to be 5 and 14 Euros/GJ, respectively. The value for selling excess heat is regarded low at 1 Euro/GJ since the location of the plant is not addressed [8]. The assumptions on the cost and performance of the electrolyzers have been taken from the report prepared by IEA about the future of hydrogen for G20 summit in Japan [53]. The MCEC electrolyzer assumptions are based on the Solid Oxide Electrolyzer Cell (SOEC) values due to similarity in the technologies as per [14]. For techno-economic analysis of the electrolyzers normalized costs based on the flow of hydrogen have been taken from [53].

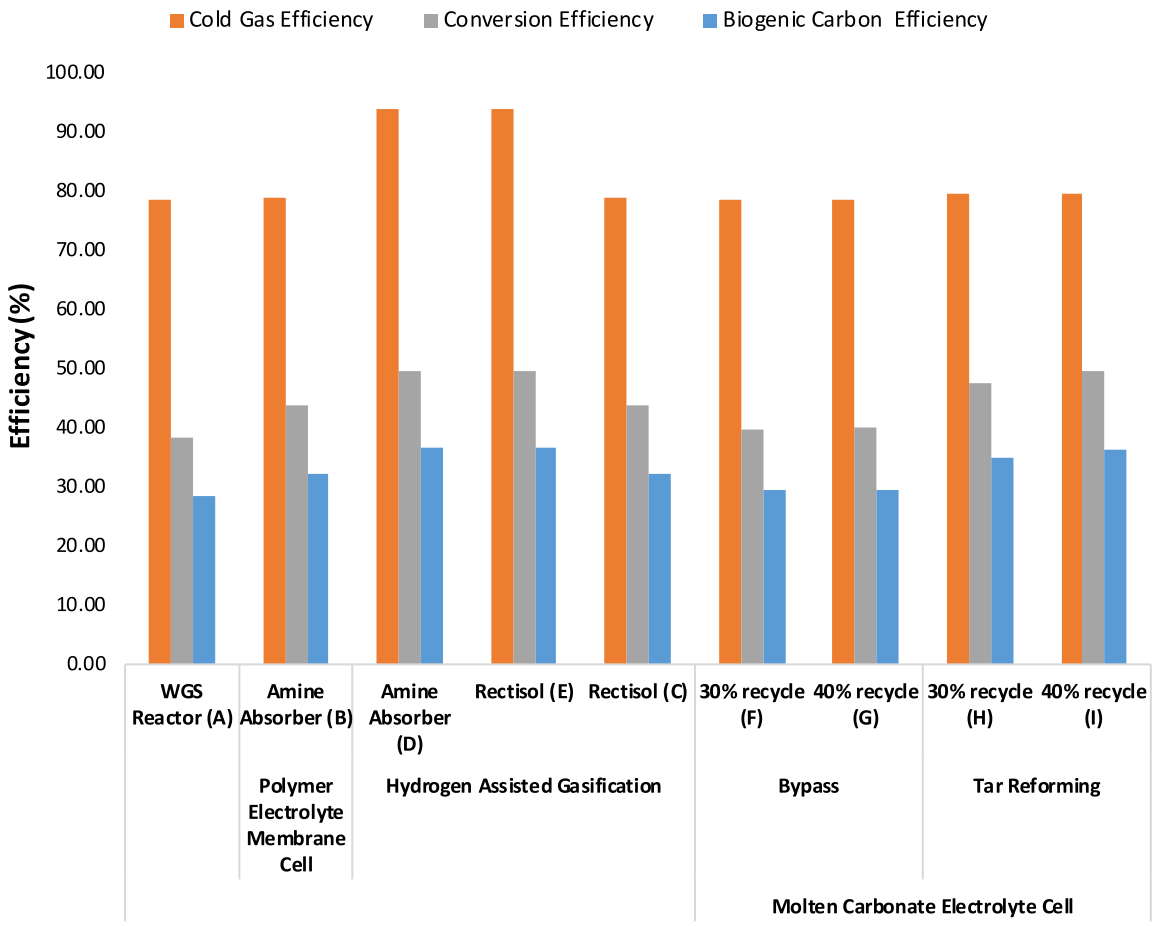

Fig. 8. Biogenic carbon efficiencies for different BtL process configurations.

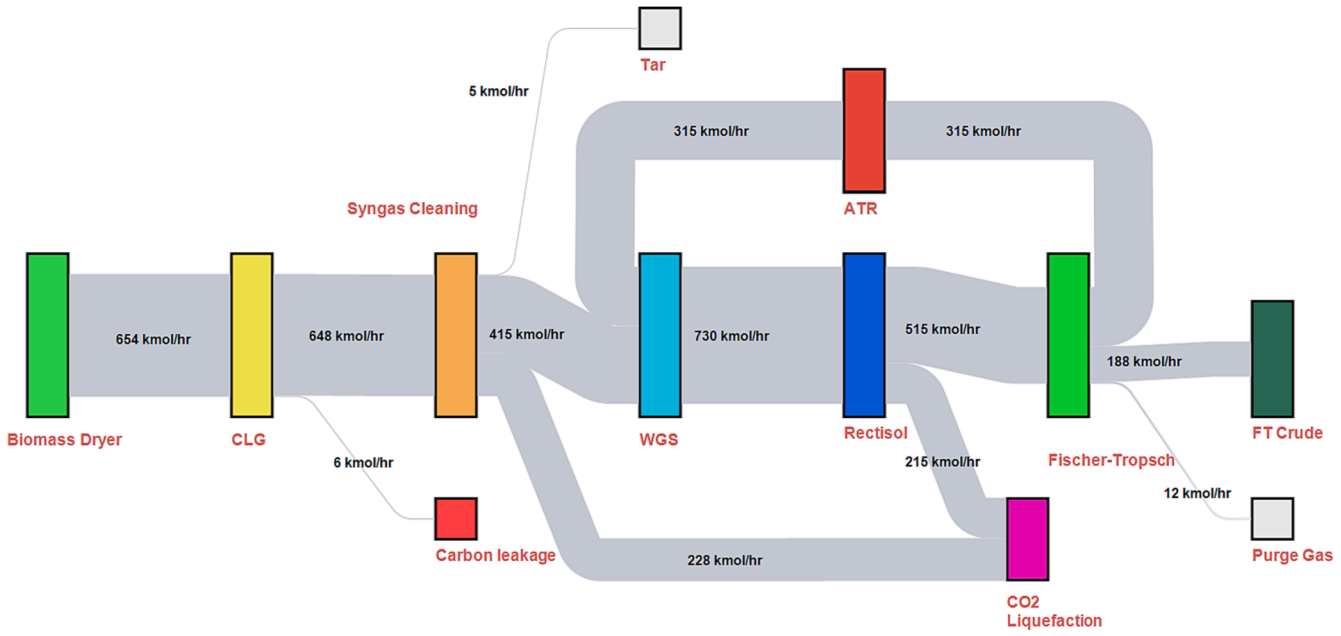

Fig. 9. Carbon flow Sankey diagram for the BtL plant with WGS reactor for syngas conditioning – Case A.

2.3.1. *Expenditure*

The total yearly cost includes the annual capital cost, which is often paid back to the bank as a yearly payment of the loan obtained from the bank for building and erecting the plant, as well as the annual O&M, fuel, and power costs.

2.3.1.1. Capital cost. Based on the literature, an estimate of the process equipment's capital cost is made. Hannula et al. [46] and Saeed et al. [8]

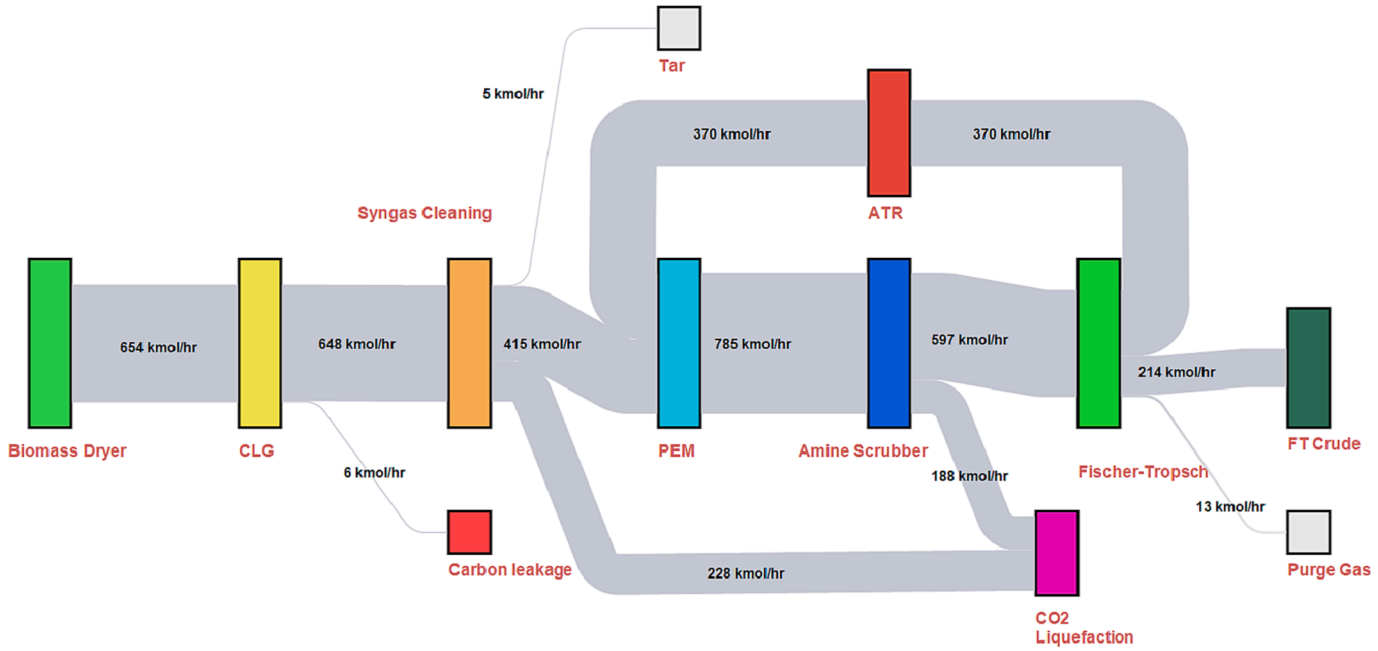

Fig. 10. Carbon flow Sankey diagram for BtL plant with syngas conditioning using hydrogen from PEM electrolyzer and amine scrubber for carbon capture – Case B.

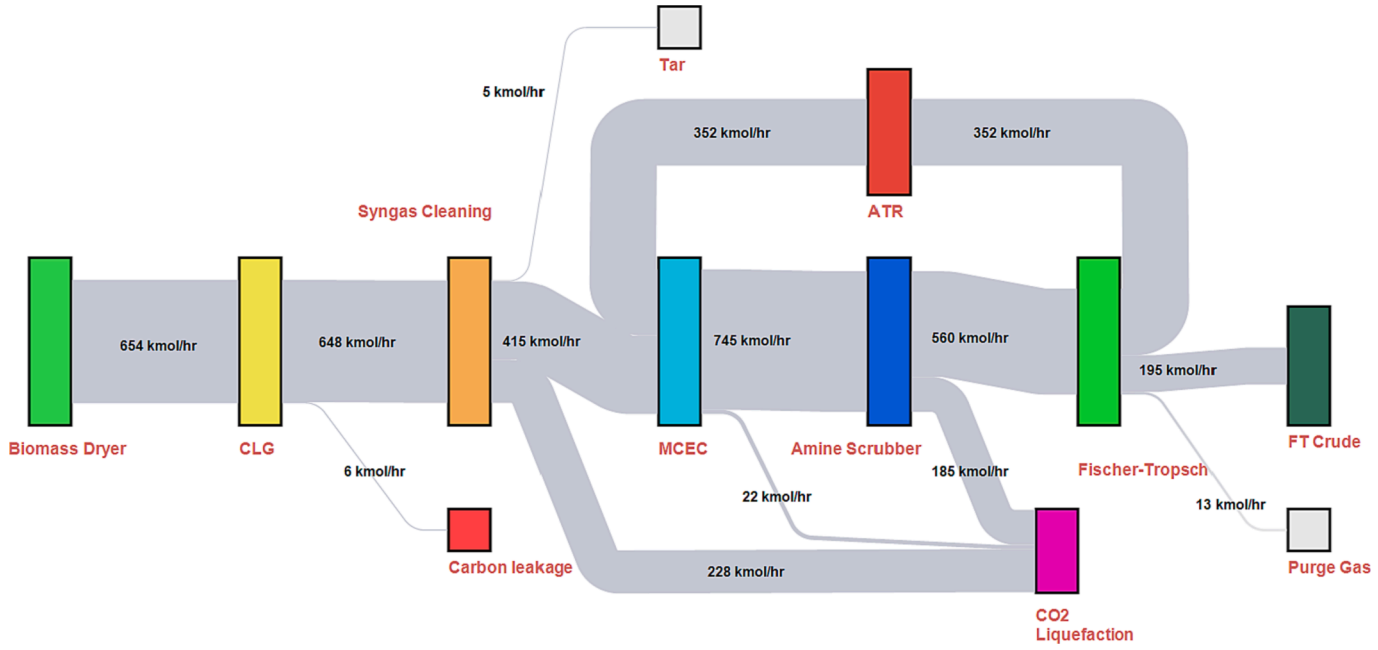

Fig. 11. Carbon flow Sankey diagram for BtL plant with syngas conditioning using MCEC electrolyzers and amine scrubber for carbon capture – Case F.

are used as the source for various reference costs and literature values used in the calculation of TPI. Using the following equation, the capital costs of the equipment are scaled up or down in accordance with the size requirements based on the model estimates.

$$C = C_0 * (\frac{S}{S_0})^f \tag{2.4}$$

where C_o (reference cost) is the price for the same equipment listed in the literature for the size S_o, and C is the price for the size S that the model suggests. Depending on the technological maturity and the year used as the reference for cost computation, the scaling factor f typically ranges between 0.6 and 0.8. The exponent is predicted to be 0.6 for most established technologies, and 0.8 for new apparatus and technologies [55].

The maximum size of equipment typically has a limit. If the maximum size of the needed piece of equipment exceeds the upper limit, numerous trains of the same piece of equipment are built so that no train surpasses the maximum size. The following calculation is used to determine the cost of the equipment for many trains of the same item:

$$C_m = C^* n^m \tag{2.5}$$

In this equation, n stands for the number of trains, while m is an exponent, typically taken to be 0.9 [55–57].

The Chemical Engineering Plant Cost Indices (CEPCI), which measure inflation, are then used to alter the costs for March 2022:

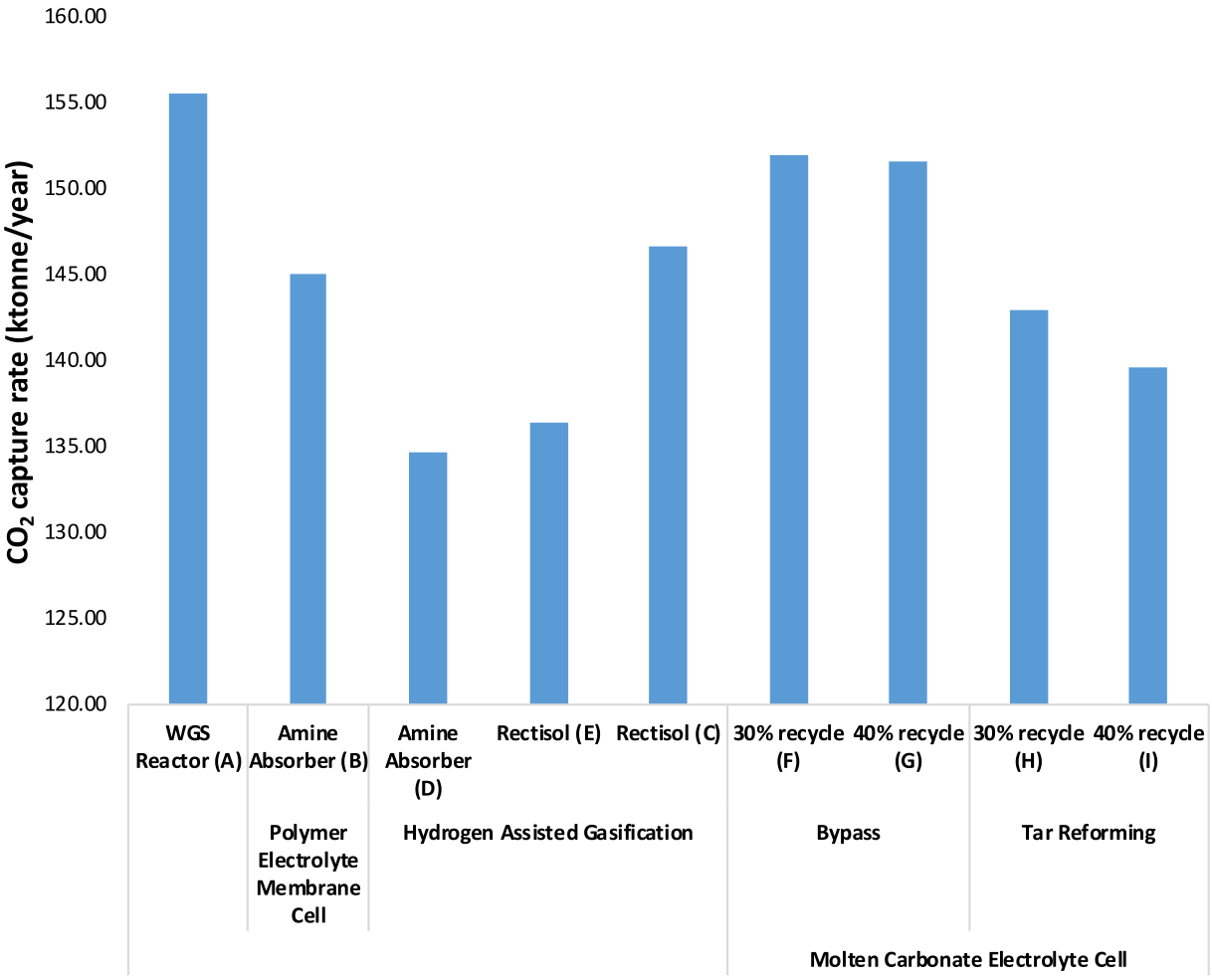

Fig. 12. CO_2 capture rate for different BtL configurations.

$$Component\ Cost_{year\ y} = Component\ Cost_{year\ x} * \frac{CEPCI_{year\ y}}{CEPCI_{year\ x}} \tag{2.6}$$

The expenses are further adjusted to account for direct costs such as plumbing, electricity, utilities, off-sites, equipment erection, structures, and site preparation after size and inflation adjustments. These expenses are frequently reported with the reference cost C_o and are known as the Balance of Plant (BOP) cost in most literature [55].

Indirect Costs (IC), which include charges for engineering, headquarters, start-up, and contingency, are also included in the component cost because they are necessary for the process's overall operation and execution.

Since the BOP and IC are typically stated as a percentage of the component cost, the usual formula to determine the Total Plant Cost (TPC) is the sum of the component costs, BOP, and IC [58]:

$$TPC = \sum_{1}^{n} C + \left(\sum_{1}^{n} C*BOP\%\right) + \left(\sum_{1}^{n} C*IC\%\right) \tag{2.7}$$

Finally, TPI is calculated using Interest During Construction (IDC), which is typically calculated as 10% of the Total Plant Cost (TPC) [59].

$$TPI = TPC*(1 + IDC) \tag{2.8}$$

To account for the capital expenditures of smaller equipment, such as pumps, heat exchangers, and tiny compressors (for pressure loss makeup), an additional 10% of overhead is added to TPI.

TPI multiplied by the Capital Recovery Factor (CRF), or annuity factor, yields the annual capital cost:

$$Annual\ Capital\ Cost = TPI*CRF \tag{2.9}$$

where CRF is the Capital Recovery Factor, calculated as follows using the plant's economic lifetime T and the discount rate r:

$$CRF = \frac{r}{1 - (1 - r)^{-T}} \tag{2.10}$$

2.3.1.2. Operations and maintenance cost. There are four categories of O&M costs:

- Personal costs
- Maintenance, and insurance of plant equipment
- Loading and replacement of catalysts and chemicals.
- Loading and makeup of oxygen carriers

According to Saeed et al. [8], the annual personnel costs, maintenance and insurance costs, and catalysts and chemicals costs are each considered as 0.5%, 2.5%, and 1% of the Total Plant Cost (TPC), respectively. It is expected that the annual oxygen carrier cost will be 1% of the TPC.

2.3.1.3. Energy cost. The expected yearly running hours, prices for biomass and electricity (shown in Table 8), as well as the corresponding energy demands that may be derived from the model, are used to determine the annual biomass and electricity expenses.

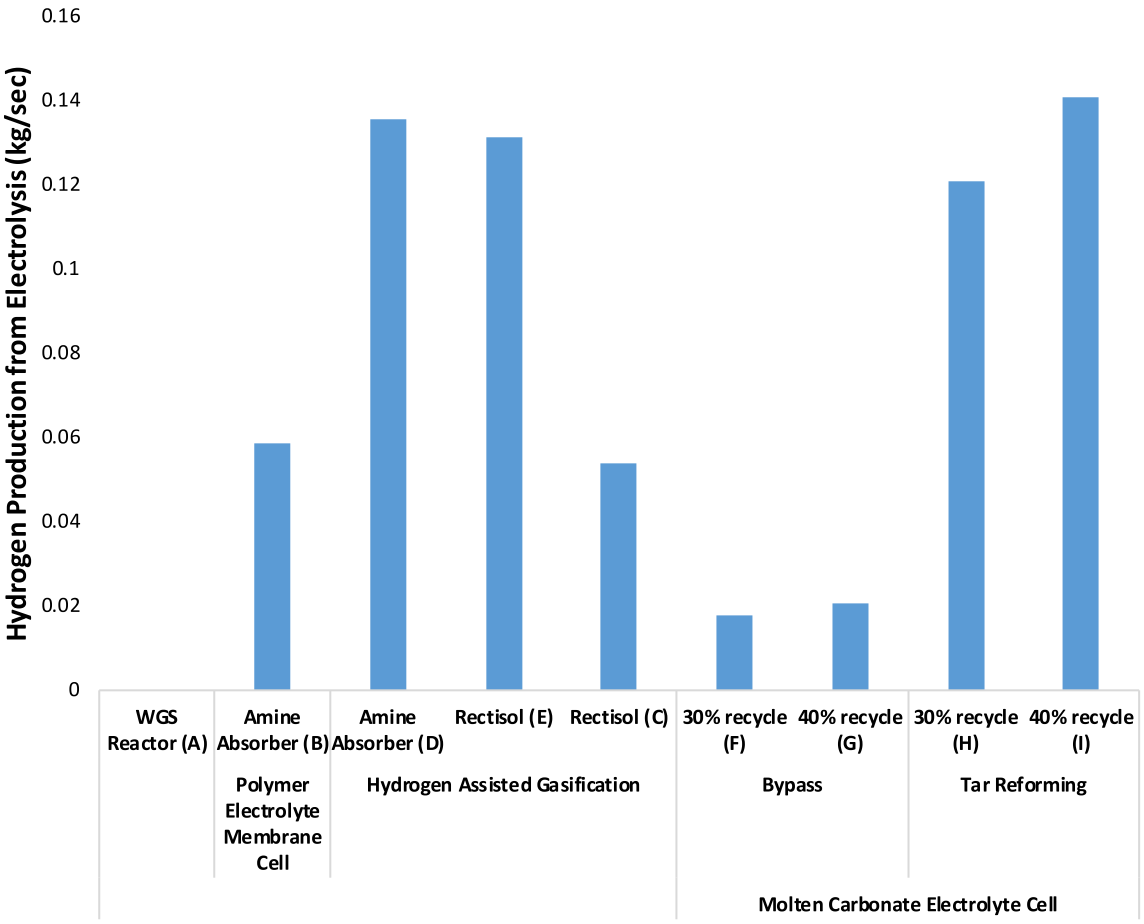

Fig. 13. Hydrogen consumption for syngas conditioning.

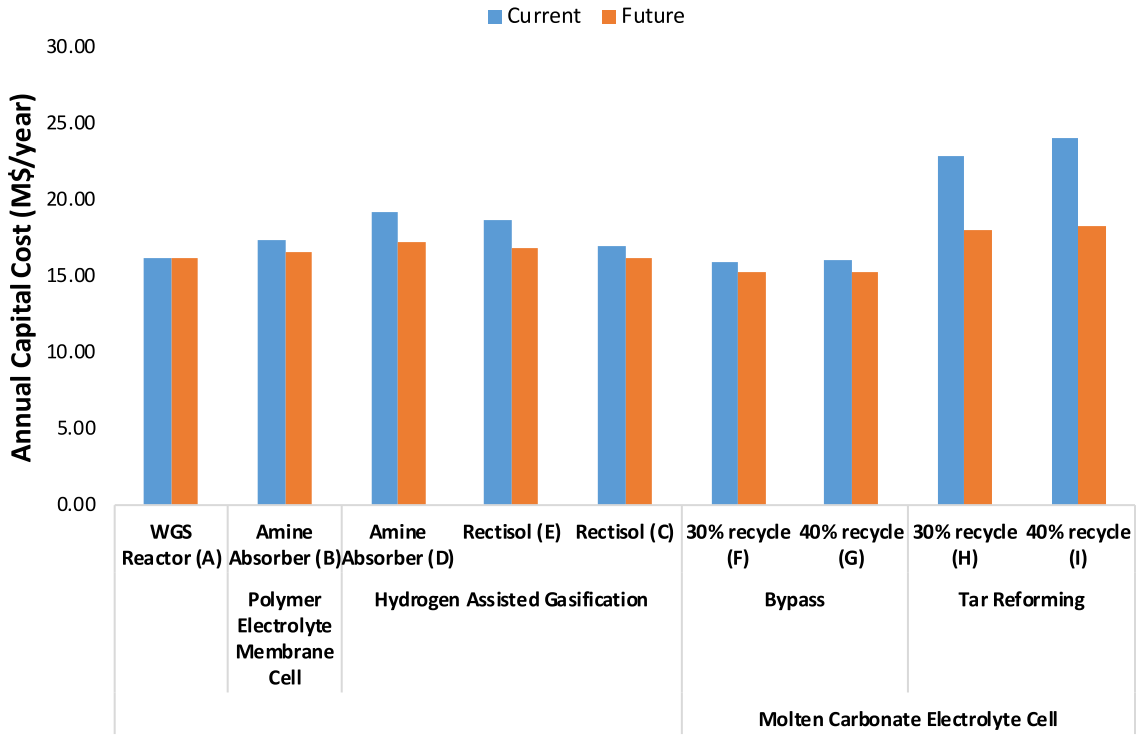

Fig. 14. Annual capital cost for BtL configuration with current and future scenarios.

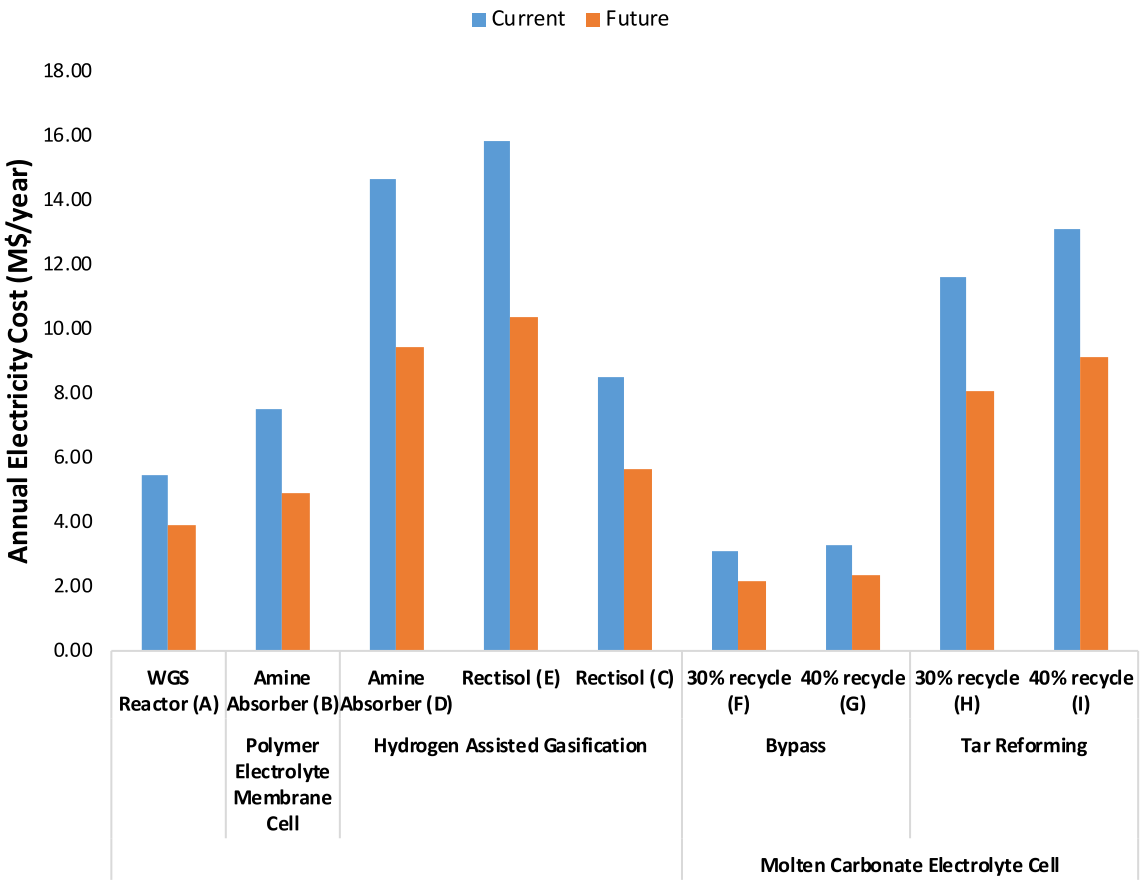

Fig. 15. Annual electricity costs for BtL plant configurations with current and future scenarios.

2.3.2. Revenue

The BtL plant sells its fuel products at pricing based on the March 2022 market's average given in Table 9. Additionally, any excess heat generated by the plant may be sold to any type of cogeneration facility, such as a district heating (DH) provider. For the plant, pinch analysis is used to determine the extra heat that is accessible. For better understanding, the grand composite curves from the pinch analysis for all the process configurations have been added in a supplementary document.

The fractions of fuel from the CDU may need to go through extra upgrading procedures since they don't completely match the standards of commercial fuels. However, FT crude is 130–180% more valuable than crude oil and is free of sulfur, nitrogen, and heteroatoms [33], [71]. As a result, it is considered that the fuel fractions in this study are of excellent quality and suitable for usage in commercial and industrial settings. The Aspen Plus model's output of a certain fuel and the associated fuel price are used to determine the revenue from the fuel.

2.3.3. Economic parameters

The following economic metrics have been used to discuss and compare the techno-economic analysis for various configurations and settings.

2.3.3.1. Levelized cost of fuel. The Levelized Cost of Fuel (LCOF) is the price at which the product (fuel) must be sold to break even on the investment (no loss and no profit). The project is lucrative if the product is sold for more money. There is a net loss if the product is sold for less. The LCOF is defined as follows [8]:

$$LCOF\left(\frac{\$}{GJ}\right) = \frac{F + C + E + O - R}{P} \tag{2.11}$$

where, P is the annual energy production of the fuel (FT crude) in GJ, R is the annual revenue from byproducts and F, C, E and O are the annual costs of biomass, capital, electricity, operations and maintenance costs, respectively, all expressed in US dollars.

2.3.3.2. Annual profit. Total annual income minus total annual costs is defined as the annual profit.

$$Annual\ Profit(\$) = Annual\ Plant\ Revenue - Annual\ Plant\ Cost \tag{2.12}$$

2.4. Future scenario

Table 10 explains the assumptions for the techno-economic analysis based on a future scenario where electrolyzers and electricity are expected to be cheaper owing to advancements in electrolyzer technology and integration of cheaper renewable electricity into the electricity system respectively [53]. A negative emissions market has also been assumed for the future with a price similar to the average EU ETS carbon permit price for March 2022 [64].

3. Results and discussion

In this section several process and techno economic parameters for the cases explained in section 2.3 are reported and compared.

3.1. Technical performance analysis

Process parameters such as cold gas and conversion efficiencies, biogenic carbon efficiency, FT crude production and hydrogen produced by the electrolyzers are compared for different process configurations. The biogenic carbon efficiency, cold gas efficiency and conversion efficiency for the case A are 28%, 78% and 38% respectively. In comparison to the configuration with WGS reactor for syngas conditioning, the

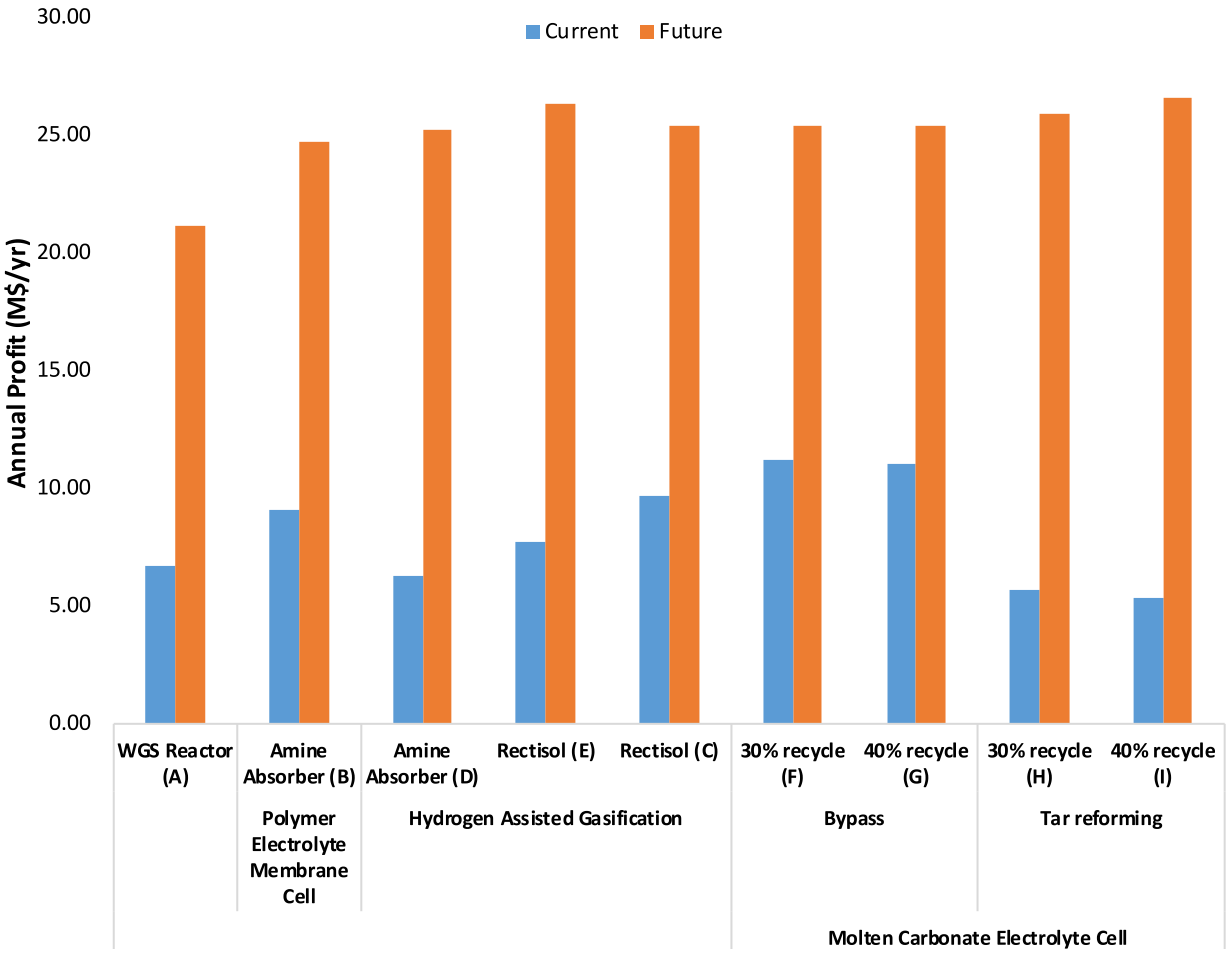

Fig. 16. Annual profits for BtL plant configurations with current and future scenarios.

configurations with PEM or MCEC electrolyzers result in better biogenic carbon and conversion efficiencies. Fig. 8 clearly shows that more biogenic carbon from the biomass ends up in the liquid fuel by the introduction of hydrogen from electrolyzers for syngas conditioning. PEM electrolyzers produce only hydrogen without WGS reaction in the cell; therefore, carbon monoxide is not consumed for conditioning the syngas [37]. On the other hand, MCEC consumes CO_2 and produces hydrogen by the reduction of water molecule, however, due to high temperatures, WGS reaction also occurs at the cathode, converting CO into CO_2 [14], which is later captured, thus resulting in lower biogenic carbon efficiencies and a lower fuel production compared to the case with PEM. The configuration where PEM electrolyzer also provides some hydrogen to the FR for assisting in gasification, the biogenic carbon efficiency increases considerably because due to the introduction of hydrogen in FR, the WGS equilibrium shifts and the reaction proceeds in reverse direction increasing CO production. It is also noted that the process configuration with Rectisol for acid gas removal (cases C and E) have slightly better biogenic carbon efficiencies than the process configuration with Amine scrubber (cases B and D). This is because less carbon dioxide is captured and removed from cases C and E compared to cases B and D owing to less carbon dioxide recycling with the FT tail gases. Moreover, with the introduction of tar reformer alongside MCEC, there is a big jump in the biogenic carbon efficiency since the biogenic carbon in the tar is not wasted and yields to more liquid fuel after conversion into syngas. Also, a higher CO_2 recycle ratio in MCEC results in a better biogenic carbon efficiency due to higher hydrogen production and lesser WGS activity. Syngas conditioning with PEM electrolyzer results in the better carbon conversion compared to that with WGS reactor or MCEC electrolyzer (without tar reforming).

Cold gas efficiencies for all the configurations are the same except for the configurations where hydrogen is introduced in the FR for assisting in gasification which also result in better cold gas efficiencies.

Figs. 9, 10 and 11 clearly show the flow of carbon utilizing three different technologies (WGS reactor, PEM electrolyzer and MCEC electrolyzer) for conditioning the syngas for optimum conversion in the FT reactor. For carbon molar flow of 654 kmol/hr as fuel in each case, 443 kmol/hr, 416 kmol/hr and 435 kmol/hr of carbon gets removed in the form of carbon dioxide in cases A, B and F accounting for 67.7%, 63.6% and 66.5% of the inlet carbon flow, respectively. The Sankey diagram also indicates that 14% and 4% more carbon ends up in FT crude for cases B and F respectively compared to case A.

Fig. 12 shows the rate of carbon captured for different BtL plant configurations in ktonne/year. It can be seen that the cases with lowest biogenic carbon efficiencies have the highest carbon capture rates and vice versa. Fig. 12 displays the CO_2 capture rates for various BtL configurations. The case A has the highest capture rate among all the configurations which shows the more carbon is lost in form of CO_2 and sent to CO_2 capture unit. However, configurations with PEM and MCEC electrolyzers show less capture rate therefore more carbon ends up into the fuel. As less CO_2 is produced during the gasification compared to other BtL process with electrolyzers, the configuration with PEM electrolyzers and hydrogen assisted gasification show the lowest CO_2 capture rate.

The hydrogen consumption for syngas conditioning for all considered cases is shown in Fig. 13. This figure follows the trends for biogenic carbon and conversion efficiencies presented in Fig. 8 as the consumption of hydrogen is closely related to these efficiencies. The more the hydrogen introduced into the process, the better the biogenic carbon

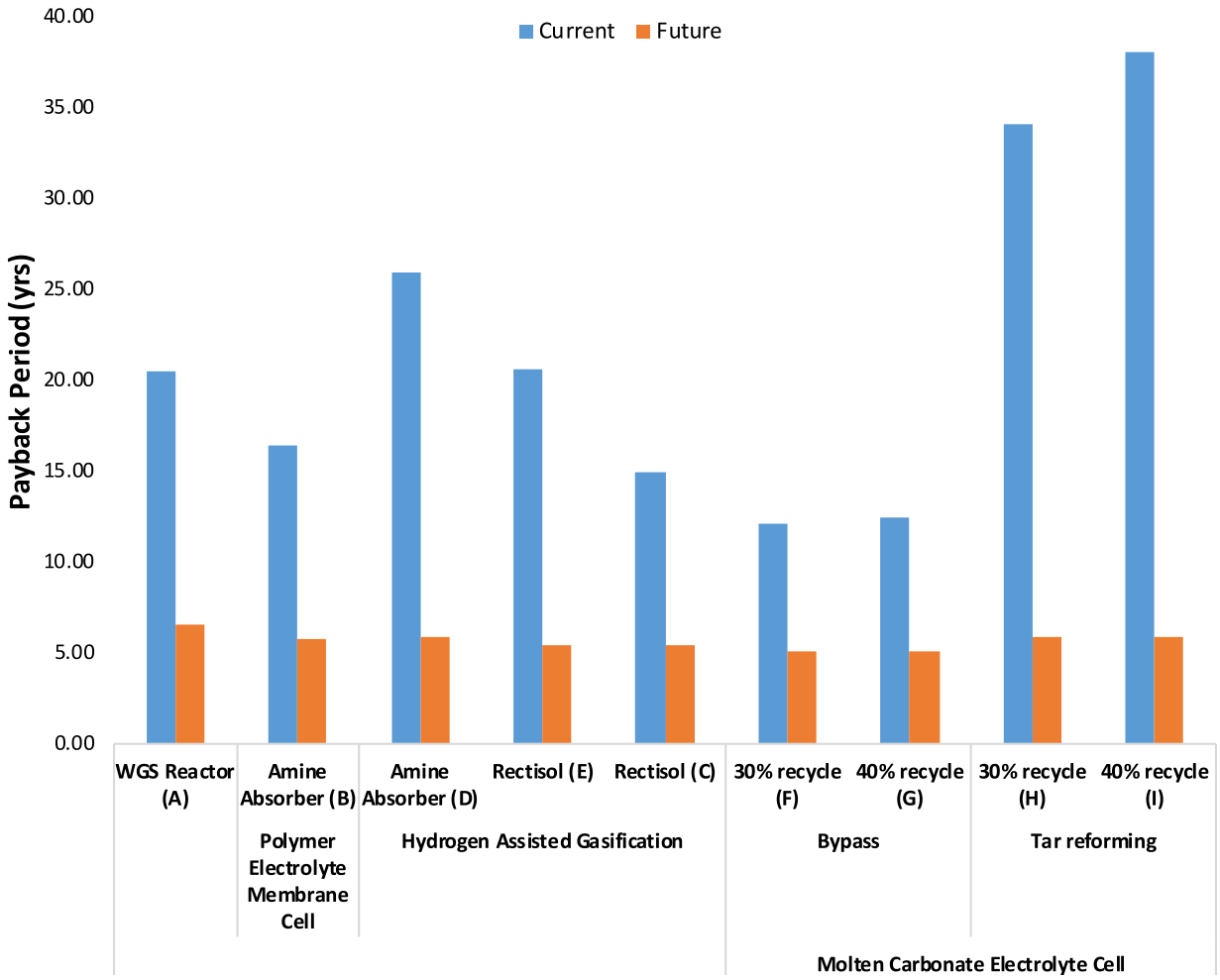

Fig. 17. Payback periods for BtL plant configurations with current and future scenarios.

and conversion efficiencies. The process models with MCEC (cases F and G) produce less hydrogen to adjust the H_2/CO ratio since the production of hydrogen is followed by WGS adjustment inside the MCEC. On the other hand, since no WGS reaction occurs in the process configurations (cases B and C) with PEM electrolyzers, more hydrogen is introduced into the process. More hydrogen is produced in the PEM to assist in gasification in cases D and E. With Amine absorber (cases B and D in Table 7), more carbon dioxide recirculates with the FT tail gases into the autothermal reformer due to lesser CO_2 captured upstream, resulting in lesser WGS activity because of equilibrium shift in the autothermal reformer and producing slightly more carbon monoxide compared to the models with Rectisol (cases C and E). This means slightly more hydrogen is needed for conditioning the syngas (before FT reactor) for the cases with Amine Absorber compared to those with Rectisol. Also, as explained earlier, a higher recirculation of CO_2 in MCEC results in higher production of hydrogen. Moreover, due to tar reformer, the syngas yield increases, however, the increase in CO yield is more than that of H_2 resulting in a drop in the H_2/CO ratio. This means that more hydrogen needs to be produced for conditioning the syngas for the desired molar ratio of H_2 and CO.

3.2. Techno-economic analysis

Most of the components in all the process configurations remain the same as case A meaning that the capital costs don't differ much, however, the introduction of electrolyzers in place of a WGS reactor usually results in an increase in the capital cost due to high equipment and installation cost for the electrolyzers. As seen in Fig. 14, the process models with MCEC and bypass (cases F and G) have slightly lower capital costs than the model with WGS reactor (case A) due to the need of a very small MCEC electrolyzers (evident from Fig. 13) for syngas conditioning since MCEC electrolyzer produces hydrogen and has WGS activity happening at cathode.

The highest costs are for process configurations with tar reformers (cases H and I), due to increased flow of syngas after the reformer resulting in need of larger components downstream, thus increasing the total capital cost. For process configurations with amine absorbers (cases B and D), more carbon dioxide recirculates with FT tail gases compared to those with Rectisol (cases C and E) which means slightly bigger FT reactors and autothermal reformers are needed, resulting in slightly higher annual capital costs. Same trend is observed for process configurations with MCEC electrolyzers (cases F to I); a higher recycle ratio results in higher flow out of MCEC, resulting in slightly bigger equipment downstream, hence slightly increasing the cost. Due to projected lower electrolyzers costs and higher efficiencies in the future (cheaper and smaller electrolyzers), the total annual cost drops for the future scenario.

The trends for both the current and future scenarios in Fig. 15 are similar to those in Figs. 8 and 13. Increased utilization of hydrogen from electrolyzers in the process results in better biogenic carbon efficiencies, but also increases the cost of electricity for the plant. The future scenario has lower electricity costs compared to the current scenario due to lower electricity prices and better electrolyzer efficiencies. Figs. 16 and 17 show that currently due to the need of a small MCEC electrolyzer

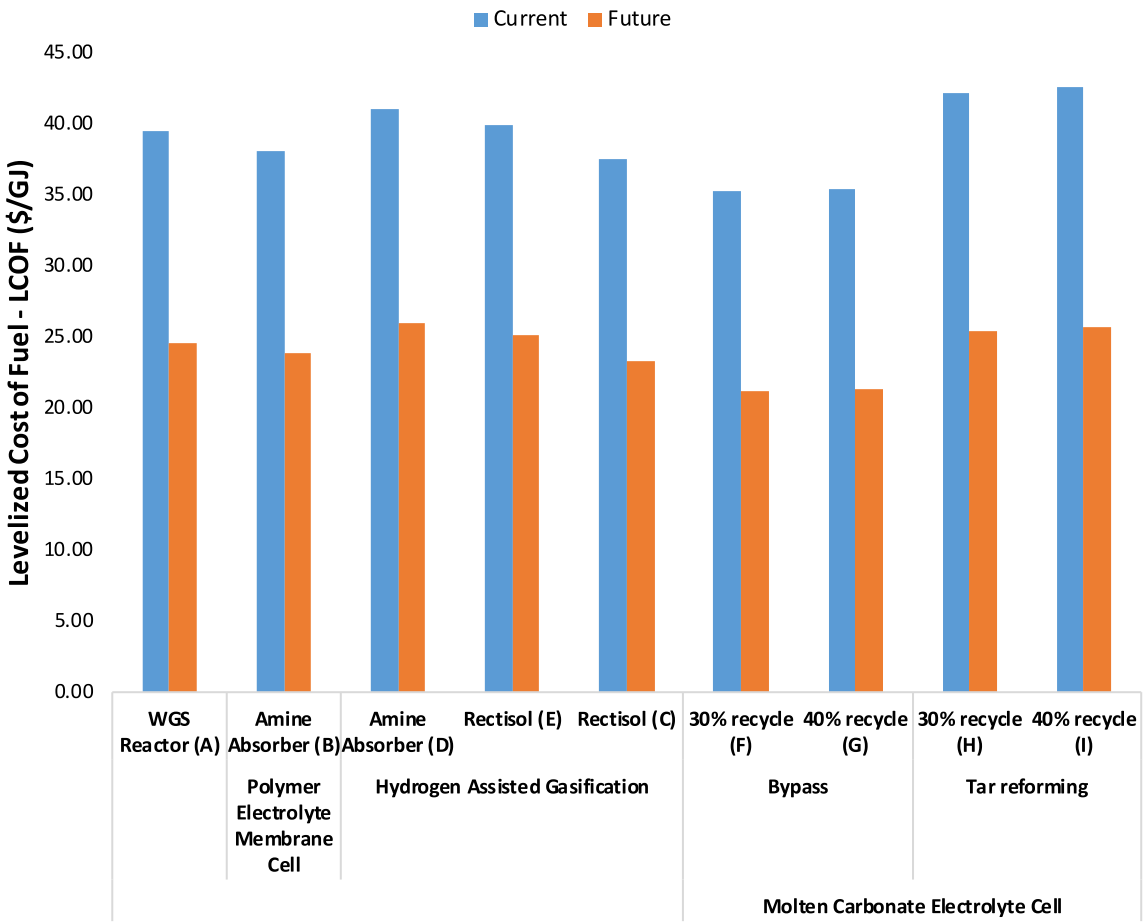

Fig. 18. Levelized cost of fuel for different BtL configurations.

consuming less electricity, cases F and G give the highest annual profit and shortest payback period, whereas process configurations with tar reforming (cases H and I) result in the least profit and longest payback period due to high cost of electrolyzer and electricity owing to high production of hydrogen.

Also, the base case (case A) has a small profit due to poor yield of liquid fuel owing to a low biogenic carbon efficiency. The process configurations with hydrogen assisted gasification (cases D and E) have lesser annual profits than cases F and G (despite having better fuel yields) because of higher capital costs. In the future, due to cheaper electricity and technological advancements in the electrolyzer technologies (better efficiencies and cheaper equipment) as assumed in the study, cases H and I result in the highest annual profits whereas case A has the lowest annual profit.

Fig. 18 that shows the levelized cost of fuel (LCOF) for different BtL processes for current and future scenarios has a similar trend to those in Figs. 16 and 17. Currently, cases F and G with MCEC and a bypass have the lowest LCOF (highest profit and shortest payback period) among all the configurations while process configurations with tar reformer (cases H and I) have the highest LCOF (lowest profit and longest payback period). In the future, case F is predicted to have the lowest LCOF whearas case D will have the highest LCOF.

4. Conclusion

Gasification could provide a viable route for conversion of biomass to liquid fuels. Still, previous works have shown limited carbon conversion and efficiencies for BtL processes using gasification techniques, which are problematic with respect to the limited resource base. This study assesses the chemical looping gasification and sustainable hydrogen addition to BtL as a novel technology to increase biogenic carbon efficiency using iron sand as OC. There haven't been any prior process studies using this material, although it is produced in huge quantities in Sweden and throughout Europe at extremely low costs and with readily accessible value chains. The results indicate that hydrogen production from electrolyzers is a viable alternative for syngas conditioning by reducing WGS activity in the process. It can clearly be seen that the models with PEM and MCEC electrolyzers have better yields of liquid fuel and biogenic carbon efficiencies compared to the base case; up to 11.5 % increase in conversion efficiency and up to 8.1 % increase in biogenic carbon efficiency. MCEC reduces water molecules to create hydrogen while consuming CO_2. In addition, the WGS reaction, which turns CO into CO_2, also takes place at the cathode because of the high temperatures which means the biogenic carbon efficiency will be lower compared to the process configurations with PEM electrolyzers; around 3 % drop in biogenic carbon efficiency for process configurations with MCEC compared to those with PEM electrolyzers. Other possible ways to increase the liquid fuel yield and the biogenic carbon efficiency are the introduction of hydrogen in FR for assisting in gasification and implementation of a tar reformer in the BtL process resulting in up to 8 % and 7 % increase in biogenic carbon efficiencies, respectively, compared to the base case.

Better biogenic carbon efficiencies are achieved by increased use of hydrogen from electrolyzers resulting in increased revenues from the liquid fuel, however, the plant's capital and power costs also rise as a result. Under assumed economic parameters, the techno-economic assessment of future cases reveals a considerable potential in integration of renewable electricity into biofuel production in which the Levelized Cost of Fuel would decrease up to 40% (up to 4 times increase in annual profit). However, the uncertainty about electricity price may

alter the techno-economic feasibility.

Funding source

We would like to acknowledge the financial support for this project from the Swedish Energy Agency (Project P51430-1).

CRediT authorship contribution statement

Mohammad Shahrivar: Methodology, Software, Validation, Resources, Data curation, Writing – original draft, Writing – review & editing, Visualization. **Muhammad Nauman Saeed:** Methodology, Software, Validation, Resources, Data curation, Writing – original draft, Writing – review & editing, Visualization. **Gajanan Dattarao Surywanshi:** Resources, Writing – review & editing, Supervision. **Tobias Mattisson:** Conceptualization, Writing – review & editing, Supervision, Project administration, Funding acquisition. **Amir H. Soleimanisalim:** Conceptualization, Investigation, Writing – review & editing, Supervision, Funding acquisition.

Declaration of Competing Interest

The authors declare that they have no known competing financial interests or personal relationships that could have appeared to influence the work reported in this paper.

Data availability

Data will be made available on request.

Appendix A. Supplementary data

Supplementary data to this article can be found online at https://doi.org/10.1016/j.fuel.2023.128525.

References

[1] Barney Jeffries and Evan Jeffries, "WILDLIFE IN A WARMING WORLD," Apr. 2018. [Online]. Available: www.swim2birds.co.uk.
[2] V. Masson-Delmotte *et al.*, "Global warming of 1.5°C: An IPCC special report on the impacts of global warming of 1.5°C," 2019. Accessed: Oct. 20, 2022. [Online]. Available: https://www.ipcc.ch/sr15/.
[3] Gasser T, Guivarch C, Tachiiri K, Jones CD, Ciais P. Negative emissions physically needed to keep global warming below 2°C. Nat Commun Aug. 2015;6. https://doi.org/10.1038/ncomms8958.
[4] The European Environment Agency (EEA), "Greenhouse gas emissions from transport in Europe," *EEA*, Nov. 18, 2021. https://www.eea.europa.eu/ims/greenhouse-gas-emissions-from-transport (accessed Oct. 11, 2022).
[5] Jacob Teter and Hyeji Kim, "Aviation," *IEA*, 2022. https://www.iea.org/reports/aviation (accessed Oct. 05, 2022).
[6] Henrik Thunman, *GoBiGas demonstration-a vital step for a large-scale transition from fossil fuels to advanced biofuels and electrofuels*. Accessed: Sep. 13, 2022. [Online]. Available: https://www.chalmers.se/SiteCollectionDocuments/SEE/News/Popularreport_GoBiGas_results_highres.pdf.
[7] S. Solomon, *Climate change 2007 : The Physical Science Basis*. Cambridge University Press, 2007. Accessed: Oct. 20, 2022. [Online]. Available: https://www.cambridge.org/se/academic/subjects/earth-and-environmental-science/climatology-and-climate-change/climate-change-2007-physical-science-basis-working-group-i-contribution-fourth-assessment-report-ipcc?format=PB&isbn=9780521705967#contentsTabAnchor.
[8] Saeed MN, Shahrivar M, Surywanshi GD, Kumar TR, Mattisson T, Soleimanisalim AH. Production of aviation fuel with negative emissions via chemical looping gasification of biogenic residues: Full chain process modelling and techno-economic analysis. Fuel Process Technol Mar. 2023;241:107585. https://doi.org/10.1016/j.fuproc.2022.107585.
[9] Isaksson J, Åsblad A, Berntsson T. Pretreatment methods for gasification of biomass and Fischer-Tropsch crude production integrated with a pulp and paper mill. Clean Technol Environ Policy 2014;16(7):1393–402. https://doi.org/10.1007/s10098-014-0815-7.
[10] A.P.Steynberg and M.E. Dry, *Fisher-Tropsch Technology*, 1st ed., vol. 152. Elsevier, 2004. Accessed: Oct. 20, 2022. [Online]. Available: https://www.sciencedirect.com/bookseries/studies-in-surface-science-and-catalysis/vol/152/suppl/C.
[11] C. Panoutsou and K. Maniatis, "Sustainable-Biomass-Availability-in-the-EU-Part-I-and-II-final-version," 2021.
[12] Bos MJ, Kersten SRA, Brilman DWF. Wind power to methanol: Renewable methanol production using electricity, electrolysis of water and CO2 air capture. Appl Energy 2020;264:114672.
[13] A. B. T. Nelabhotla, D. Pant, and C. Dinamarca, "Power-to-gas for methanation," in *Emerging Technologies and Biological Systems for Biogas Upgrading*, Elsevier, 2021, pp. 187–221. doi: 10.1016/B978-0-12-822808-1.00008-8.
[14] Mesfun S, Engvall K, Toffolo A. Electrolysis Assisted Biomass Gasification for Liquid Fuels Production. Front Energy Res Jun. 2022;10. https://doi.org/10.3389/fenrg.2022.799553.
[15] C. Breyer, E. Tsupari, V. Tikka, and P. Vainikka, "Power-to-gas as an emerging profitable business through creating an integrated value chain," in *Energy Procedia*, Elsevier Ltd, 2015, pp. 182–189. doi: 10.1016/j.egypro.2015.07.668.
[16] Boliden, Jarnsand Accessed Oct. 17, 2022. [Online]. Available: https://www.boliden.com/globalassets/operations/products/by-products/335-7128-jarnsand-produktblad_en5.pdf.
[17] Condori O, García-Labiano F, de Diego LF, Izquierdo MT, Abad A, Adánez J. Biomass chemical looping gasification for syngas production using LD Slag as oxygen carrier in a 1.5 kWth unit. Fuel Process Technol 2021;222:106963.
[18] Clara project, "Chemical Looping Gasification," 2020. https://clara-h2020.eu/chemical-looping-gasification/ (accessed Oct. 05, 2022).
[19] A. Hedayati, A. H. Soleimanisalim, C. J. Linderholm, T. Mattisson, and A. Lyngfelt, "Experimental evaluation of manganese ores for chemical looping conversion of synthetic biomass volatiles in a 300 W reactor system," *J Environ Chem Eng*, vol. 9, no. 2, Apr. 2021, doi: 10.1016/j.jece.2021.105112.
[20] Hedayati A, Soleimanisalim AH, Mattisson T, Lyngfelt A. Thermochemical conversion of biomass volatiles via chemical looping: Comparison of ilmenite and steel converter waste materials as oxygen carriers. Fuel 2022;313:122638.
[21] Andersson V, Soleimanisalim AH, Kong X, Leion H, Mattisson T, Pettersson JBC. Alkali interactions with a calcium manganite oxygen carrier used in chemical looping combustion. Fuel Process Technol 2022;227:107099.
[22] Gogolev I, Soleimanisalim AH, Mei D, Lyngfelt A. Effects of Temperature, Operation Mode, and Steam Concentration on Alkali Release in Chemical Looping Conversion of Biomass-Experimental Investigation in a 10 kWthPilot. Energy Fuel Sep. 2022;36(17):9551–70. https://doi.org/10.1021/acs.energyfuels.1c04353.
[23] Marx F, Dieringer P, Ströhle J, Epple B. Design of a 1 MWth pilot plant for chemical looping gasification of biogenic residues. Energies (Basel) May 2021;14(9). https://doi.org/10.3390/en14092581.
[24] O. Condori, F. García-Labiano, L. F. de Diego, M. T. Izquierdo, A. Abad, and J. Adánez, "Syngas production via Biomass Chemical Looping Gasification (BCLG) in a 50 kW th unit using ilmenite as oxygen carrier," 2022.
[25] Ge H, Guo W, Shen L, Song T, Xiao J. Experimental investigation on biomass gasification using chemical looping in a batch reactor and a continuous dual reactor. Chem Eng J Feb. 2016;286:689–700. https://doi.org/10.1016/j.cej.2015.11.008.
[26] Hildor F, Soleimanisalim AH, Seemann M, Mattisson T, Leion H. Tar characteristics generated from a 10 kWth chemical-looping biomass gasifier using steel converter slag as an oxygen carrier. Fuel Jan. 2023;331:125770. https://doi.org/10.1016/j.fuel.2022.125770.
[27] A. H. Soleimanisalim, F. Hildor, D. Mei, I. Gogolev, and T. Mattisson, "Selection of oxygen carrier for chemical looping gasification of biomass," 24th Fluidized Bed Conversion Conference, Gothenburg, 2022.
[28] Condori O, García-Labiano F, de Diego LF, Izquierdo MT, Abad A, Adánez J. Biomass chemical looping gasification for syngas production using ilmenite as oxygen carrier in a 1.5 kWth unit. Chem Eng J 2021;405:126679.
[29] Frilund C, Tuomi S, Kurkela E, Simell P. Small- to medium-scale deep syngas purification: Biomass-to-liquids multi-contaminant removal demonstration. Biomass Bioenergy 2021;148:106031.
[30] Arvidsson M, Morandin M, Harvey S. Biomass gasification-based syngas production for a conventional oxo synthesis plant-process modeling, integration opportunities, and thermodynamic performance. Energy Fuel Jun. 2014;28(6):4075–87. https://doi.org/10.1021/ef500366p.
[31] H. Boerrigter and H. Uil, "Green diesel from biomass via Fischer-Tropsch synthesis: New insights in gas cleaning and process design," *Green Diesel from Biomass Via Fischer-Tropsch Synthesis: New Insights in Gas Cleaning and Process Design*, Jan. 2003.
[32] Barbieri G. "Water Gas Shift (WGS)", in *Encyclopedia of Membranes*, Springer. In: Drioli E, Giorno L, editors. Encyclopedia of Membranes. Berlin, Heidelberg: Springer Berlin Heidelberg; 2015. p. 1–4.
[33] Eurosat, "Shedding light on energy in the EU A GUIDED TOUR OF ENERGY STATISTICS 2," 2021.
[34] Smith O, Cattell O, Farcot E, O'Dea RD, Hopcraft KI. The effect of renewable energy incorporation on power grid stability and resilience. Sci Adv 2022;8(9).
[35] E. Taibi, R. Miranda, W. Vanhoudt, T. Winkel, J.-C. Lanoix, and F. Barth, *Hydrogen from renewable power: Technology outlook for the energy transition*. 2018. [Online]. Available: www.irena.org.
[36] Pinsky R, Sabharwall P, Hartvigsen J, O'Brien J. Comparative review of hydrogen production technologies for nuclear hybrid energy systems. Prog Nucl Energy 2020;123:103317.
[37] S. Shiva Kumar and V. Himabindu, "Hydrogen production by PEM water electrolysis – A review," *Materials Science for Energy Technologies*, vol. 2, no. 3. KeAi Communications Co., pp. 442–454, Dec. 01, 2019. doi: 10.1016/j.mset.2019.03.002.
[38] Nikolaidis P, Poullikkas A. A comparative overview of hydrogen production processes. Renew Sustain Energy Rev 2017;67:597–611.
[39] Hu L, Lindbergh G, Lagergren C. Performance and Durability of the Molten Carbonate Electrolysis Cell and the Reversible Molten Carbonate Fuel Cell. J Phys Chem C Jun. 2016;120(25):13427–33. https://doi.org/10.1021/acs.jpcc.6b04417.

[40] Davis BH. Overview of reactors for liquid phase Fischer-Tropsch synthesis. Catal Today 2002;71(3-4):249–300.
[41] Achinas S, Margry S, Euverink GJW. In: 8 - A technological outlook of biokerosene production. Academic Press; 2021. p. 225–46. https://doi.org/10.1016/B978-0-12-820297-5.00011-6.
[42] Ibarra-Gonzalez P, Rong B-G. A review of the current state of biofuels production from lignocellulosic biomass using thermochemical conversion routes. Chin J Chem Eng 2019;27(7):1523–35.
[43] Hamelinck CN, Faaij APC, den Uil H, Boerrigter H. Production of FT transportation fuels from biomass; technical options, process analysis and optimisation, and development potential. Energy 2004;29(11):1743–71. https://doi.org/10.1016/j.energy.2004.01.002.
[44] Choudhury HA, Chakma S, Moholkar VS. Biomass Gasification Integrated Fischer-Tropsch Synthesis: Perspectives, Opportunities and Challenges. In: Recent Advances in Thermochemical Conversion of Biomass. Elsevier Inc.; 2015. p. 383–435. https://doi.org/10.1016/B978-0-444-63289-0.00014-4.
[45] Song H-S, Ramkrishna D, Trinh S, Wright H. Operating Strategies for Fischer-Tropsch Reactors: A Model-Directed Study. Korean J Chem Eng 2004;21(2):308–17.
[46] Hannula I. Hydrogen enhancement potential of synthetic biofuels manufacture in the European context: A techno-economic assessment. Energy Jun. 2016;104:199–212. https://doi.org/10.1016/j.energy.2016.03.119.
[47] Hannula I. Hydrogen enhancement potential of synthetic biofuels manufacture in the European context: A techno-economic assessment. Energy 2016;104:199–212.
[48] Carl. Wilén, Antero. Moilanen, and Esa. Kurkela, *Biomass feedstock analyses*. VIT Publications, 1996. Accessed: Oct. 20, 2022. [Online]. Available: https://www.osti.gov/etdeweb/servlets/purl/434876.
[49] Larsson A, Israelsson M, Lind F, Seemann M, Thunman H. Using ilmenite to reduce the tar yield in a dual fluidized bed gasification system. Energy Fuel Apr. 2014;28(4):2632–44. https://doi.org/10.1021/ef500132p.
[50] Corella J, Toledo JM, Molina G. Performance of CaO and MgO for the hot gas clean up in gasification of a chlorine-containing (RDF) feedstock. Bioresour Technol Nov. 2008;99(16):7539–44. https://doi.org/10.1016/j.biortech.2008.02.018.
[51] Aspen Technology, "Aspen Plus 12.1 Getting Started Modeling Processes with Solids," 1981. [Online]. Available: http://www.aspentech.com.
[52] Irvin Glassman, Richard A. Yetter, and Nick G. Glumac, "Combustion," Chalmers University of Technology, 2014. doi: doi.org/10.1016/C2011-0-05402-9.
[53] Noé van Hulst, "The Future of Hydrogen," 2019.
[54] Habermeyer F, Kurkela E, Maier S, Dietrich R-U. Techno-Economic Analysis of a Flexible Process Concept for the Production of Transport Fuels and Heat from Biomass and Renewable Electricity. Front Energy Res 2021;9. https://doi.org/10.3389/fenrg.2021.723774.
[55] K. M. Holmgren, "Investment cost estimates for gasification-based biofuel production systems," Stockholm, 2015. Accessed: Sep. 13, 2022. [Online]. Available: https://www.ivl.se/download/18.7e136029152c7d48c202a1d/1465298345076/B2221.pdf.
[56] Liu G, Larson ED, Williams RH, Kreutz TG, Guo X. Making Fischer-Tropsch fuels and electricity from coal and biomass: Performance and cost analysis. Energy Fuel Jan. 2011;25(1):415–37. https://doi.org/10.1021/ef101184e.
[57] Liu G, Larson ED, Williams RH, Kreutz TG, Guo X. Online Supporting Material for Making Fischer-Tropsch Fuels and Electricity from Coal and Biomass: Performance and Cost Analysis. Energy Fuel 2011;25(1):415–37.
[58] Kreutz TG, Larson ED, Liu G, Williams RH. Fischer-Tropsch Fuels from Coal and Biomass. Pennsylvania, USA: Princeton Environmental Institute; Sep. 2008.
[59] I. Hannula, E. Kurkela, and Valtion teknillinen tutkimuskeskus, "Liquid transportation fuels via large-scale fluidised-bed gasification of lignocellulosic biomass," VTT, Espoo, Finland, 2013. Accessed: Oct. 20, 2022. [Online]. Available: https://www.researchgate.net/publication/303309834_Liquid_transportation_fuels_via_large-scale_fluidised-bed_gasification_of_lignocellulosic_biomass.
[60] Trading Economics, "Natural Gas price," 2020. tradingeconomics.com (accessed Mar. 24, 2020).
[61] Global Petrol Prices, "Gasoline and Diesel price." https://www.globalpetrolprices.com/ (accessed Mar. 21, 2022).
[62] The International Air Transport Association (IATA), "Jet A fuel price." IATA.org (accessed Mar. 18, 2022).
[63] Raha Paraffin Co., "Wax price." https://paraffinwaxco.com/ (accessed Mar. 21, 2022).
[64] EU commission, "EU Emissions Trading System (EU ETS)," Dec. 02, 2022. https://climate.ec.europa.eu/eu-action/eu-emissions-trading-system-eu-ets_en (accessed Dec. 02, 2022).